NASA Technical Memorandum 89046

LaRC CONCEPTUAL DESIGN OF SOLID ROCKET BOOSTER IN-LINE BOLTED JOINT

DECEMBER 1986

(NASA-TM-89046) LaRC CONCEPTUAL DESIGN OF SOLID ROCKET BOOSTER IN-LINE BOLTED JOINT (NASA) 89 p CSCL 01A

N87-15177

Unclas
G3/02 40311

National Aeronautics and
Space Administration

Langley Research Center
Hampton, Virginia 23665

TABLE OF CONTENTS

TABLE OF CONTENTS (cont'd)

ACKNOWLEDGEMENTS

Appreciation is extended to the following persons for their written contributions:

K. D. Hedgepeth
C. E. Gray
M. C. Lindell
W. A. Stalnaker
W. Alexander, Jr.
W. M. Berrios
D. H. Butler
A. B. Carlson
E. A. Crossley
R. B. Davis
P. B. Gregory
N. D. Watson
W. F. Hunter
T. C. Jones
W. S. Lassiter

SUMMARY

An alternate field joint design has been developed by LaRC. The design effort was limited to a period of approximately three weeks in order to meet schedule constraints imposed by NASA Headquarters. The design has not been optimized for weight reduction but has been developed with safety as the highest priority. All design requirements for the SRB have been considered in addition to the evaluation criteria developed by LaRC to assess other candidate SRB joint designs.

Design features of the joint include a bolted in-line flanged joint with two face seals, one an elastomer "O" ring and the other a metal "C" ring. These static seals are seated at installation, remain seated and can be verified by pressure testing. The joint is preloaded to prevent gapping between sealing surfaces during flight. An inner liner seal together with an interference fit of the liner faces of the two mating segments protect the joint from hot gases. The in-line bolted concept requires the bolts to be parallel to the casing causing protrusion into the propellant volumne. Also, the in-line joint weighs about 940 lb more than the clevis-tang design but the effects are minimal because the propellant loss offsets the structural weight increase. Shuttle performance is slightly altered because of the structural and propellant weight exchange.

An internal soft seal is compressed between rigid insulating rings preventing hot gases from reaching the pressure shell. Thermal analysis has shown this concept to be acceptable, even in the event of a failure in which a gap to the shell is opened. A smooth fairing covers the external surface of the joints for aerodynamic purposes and thermal protection.

A goal that was not satisfied was zero opening of the seal gap under load. Early analysis indicated that a small gap would develop at the flange sealing area of approximately .002 to .007 inches. The metallic "C" ring was included in the design to accommodate the expected flange deflection. Metallic "C" rings have sufficient low temperature response characteristics and springback margin to remain seated throughout an STS mission. Further studies (which are not complete) have indicated that the gapping can be reduced on an optimized design.

Manufacture of the new joint is within the capabilities of the vendors but will cause at least a 12-month impact to the current STS Program schedule for development of a new SRB joint.

Verification testing of the new design does not represent a major problem and in fact may be more straight forward than required by redesigned joints which utilize the same forgings. This design can be further optimized to reduce structural weight and minimize propellant loss.

INTRODUCTION

LaRC was requested by NASA Headquarters to develop a concept for the SRB field joint without the constraint of using existing forgings. An evaluation team was assembled at the LaRC and developed criteria (table 1) for an acceptable design that would meet the objectives for a safe, reliable, and analyzable joint.

The team, using the design criteria, proceeded to develop a concept in a period of three weeks. Several concepts were evaluated before the In-Line Bolted-Joint Conceptual Design (figures 1 and 2) was selected. The design contains two flanged face seals that are preloaded by bolts and remain seated. The seals selected were a metal "C" ring and a Viton elastomer "O" ring. Internal insulation protects the seals from hot motor gases and the outside of the SRB case joint is protected from aerodynamic heating by a cork covering.

The design has not been optimized and several areas need additional study and analysis (i.e., weight reduction, high stresses, and propellant volume displacement) to determine the impact on the shuttle performance. The details of this design are covered in the following sections of this report.

SRB IN-LINE JOINT CONCEPT

Configuration Description

The Space Shuttle Solid Rocket Booster (SRB) is composed of several subassemblies; the nose cone, solid rocket motor, and the nozzle assembly. Each SRB motor is made of 11 individual cylindrical weld-free sections about 12-feet in diameter. After assembly they form a cylinder about 116 feet long. The 11 sections consist of the forward dome section, six cylindrical sections, the aft external tank-attach ring section, two stiffener sections, and the aft dome sections.

The 11 sections of the SRB case are joined by tang-and-clevis joints held together by 177 steel pins around the circumference of each joint. After the sections have been machined to close tolerances and fitted, they are assembled at the factory into four segments. These four cylindrical segments are then cast with propellant and shipped to KSC for assembly. The joints assembled at the factory are called factory joints and the joints between the four propellant-filled segments are called field joints. The in-line joint concept represents a redesign of the field joint.

The SRB joint concept (figures 1 and 2) developed by the LaRC is a face sealed in-line bolted joint. (In-line indicates that the fastener centerline is parallel to the centerline of the cylindrical pressure vessel.) This concept was selected because face seals are much less prone to leakage in a dynamic environment than the gland type seals used in the existing design on STS.

The joint geometry was selected to minimize the forces and moments that tend to reduce seal effectiveness. Integral flanges are attached to the pressure casing with gussets located between the 144 fasteners. The preloaded fasteners

assure that seal area flange deflection is minimized during the ignition and burning of the SRB.

The seal configuration selected consists of a Viton elastomer "O" ring on the inside and a metallic "C" ring on the outside. It is felt that this configuration will be tolerant to the prelaunch temperature variations experienced by the STS.

A cork fairing is bonded over the in-line joint to protect the fasteners and flange from external heating and to assure that aerodynamic drag losses are minimized. A smooth bonding surface is formed by filling the void between the gussets with foam. The cork is then bonded to the cylindrical portion of the motor case as well as over the gussets and foam.

Rigid rings compressing a soft elastomer seal (figure 3) protect the SRB case and the face seals from internal heating. These rings are molded phenolic-silica and the elastomer seal is a low durometer NBR. Bonding is the proposed method for attaching the rings to the steel case and the NBR liner. The purpose of the soft seal is to fill voids that may result from manufacturing tolerances.

Thermal analysis results indicate that this concept will perform satisfactorily even if the interior 50 percent of the rings are burned away and local gap openings form. A feature of the rigid ring concept is that the gap formed between the rings and soft seal, when exposed to a temperature drop, will be extremely small when compared to the current design. The rings will remain bonded during horizontal testing and allow for propellant venting.

Design Considerations and Tradeoffs

Several configurations, components, materials, etc. were investigated for each element of the in-line bolted joint concept. Some of these considerations and tradeoffs were:

- o Joint deflection
- o Weight increase and joint gaps
- o Drag
- o Thermal protection pf seal area
  - Preloaded insulation joint interface
  - Bonded insulation joint interface
- o Bolt size and spacing, and web/flange thickness ratio
- o Materials - space qualified, if possible
- o Forging sizes - use of existing billets and minimum additional tooling
- o Handling at KSC - assembly/disassembly
- o Manufacturability - can tolerance requirements be met

Final selections evolved from a series of iterations and working level reviews comment by the design team.

Two of the alternate structural configurations that were considered are shown in figures 4 and 5. The primary variable was the location of the bolts relative to the basic pressure vessel wall. Fastener tradeoff studies considered number and size as well as bolt and nut or stud and nuts. Bolt size and spacing data are summarized in table 2.

Several flange seal variations were considered and those determined to be leading candidates are shown in table 3; materials included Viton, Inconel 718 and others. It is felt that the Viton will seal satisfactorily at -15°F when used in

face seal applications. Seal design concepts considered were solid cross section elastomer "O" rings, tubular metallic "O" rings and metallic "C" rings. Tubular metallic "O" rings were rejected because of the high loads (1200 lb/in) required for seating. "C" rings require about 450 lb/in to seat and elastomer "O" ring seating requirements are minimal for face seals.

Other liner seal concepts considered are shown in figures 6 and 7. The bonded and putty filled methods were rejected because it was felt that there could be a structural failure of the ring internal surface due to internal pressure. Also, the bonded joint would be very difficult to disassemble and the putty distribution would be hard to control at assembly. The unbonded joint was rejected because it did not address the criteria requiring that no hot gases reach the SRB case.

Table 4 contains weight comparison between the present design and the 51-L design. Details of the weight tradeoff study are discussed later.

REQUIREMENTS

General

Design Requirements utilized in the design of the in-line bolted joint; along with those of table 1 were:

- Forging thickness requirement to be less than 3.5 inches
- In the event of the internal seal failure a tortuous path greater than 2½" long between hot gas and pressure shell shall be provided
- Seal material volatile content less than that of the NBR

Loads

The loading condition analyzed in this report is associated with the SRB ignition stage, and represents the highest loading that occurs on any joint during flight. This loading condition was chosen to analyze a worst stress situation. The loads shown below occur toward the forward end of the SRB at station 531 and can be referenced in "Space Shuttle High Performance Motor SRM Case Stress Analysis", document number TWR-12968 Rev. A, Section III.1, dated January 10, 1983, prepared for NASA by the Thiokol Corporation.

1. Internal Pressure: 988 psi (1000 psi used in analysis)

   Maximum Axial Load: 17.8×10^6 lb (18×10^6 lb used)

   (includes the effect of a bending moment of 95.1×10^6 in-lb)

   See STRUCTURAL ANALYSIS section for further discussion of the loads.

2. Seal Loads

   "C" seal seating force

   450 lb/in. combined with other loads

Factors and Margins of Safety

- Factor of Safety (f.s.)
  - 1.4 on ultimate strength
  - 1.25 on yield strength
  - Bolt preload is 70 percent of ultimate strength
  - Required number of bolts is 1.5 times the number needed to balance the axial load based on the bolts being loaded to 70 percent of ultimate strength

- Margins of Safety

  ≥ 0 when computed as follows:

  $$MS = \frac{\text{allowable load}}{\text{limit load x f.s.}} - 1$$

  where the following definitions apply:

  - Limit load is the maximum expected load
  - Allowable load results from combining element section and material strength properties that have received general acceptance for use in design

Internal Environment

The hot gases produced from the burning of the SRB propellant determine the internal environment design requirements for the in-line joint. Steady state as well as dynamic effects were considered. Steady state gas temperatures, pressures, and properties are presented in table 5.

Dynamic effects considered are the result of small pressure fluctuations in the SRB during propellant burn. These acoustic pressure oscillations are 1.92 psi (0 to peak) with a predominate frequency of 15 hz as measured by NASA-MSFC. The hot gas effects are applied throughout the two-minute burn period.

In-line joint subsystems affected by lift-off noise, pressure gradients, and plume impingement were designed to be similar to, or stronger than, related items on the clevis-tang design. Maximum predicted SRB external temperatures were used to design the in-line joint fairing and heat protection because heating rate information was not available.

The temperature-time histories predicted from data supplied by MSFC are summarized below:

0 - 150 sec.; aerodynamic heating

maximum cork temperature: 375°F

maximum cork/SRB temperature: 255°F

150 - 260 sec.; cooling

260 - 310 sec.; internal heating

maximum cork temperature: 465°F

maximum cork/SRB temperature: 240°F

The maximum temperature of the exposed flange when subjected to the above conditions is predicted to be 275°F.

WEIGHT AND PROPELLANT CONFIGURATIONS

Since the weight is a major consideration of any SRB redesign, LaRC has reviewed various design options for reducing the weight. One such approach which shows promise includes the use of a larger number of smaller bolts. Due to the time allowed for this study the details on a lighter weight design have not been completed.

Weight comparisons between the proposed SRB joint redesign and the existing joint were made choosing 12 inches on either side of the case interface as a reference length. Nominal dimensions were used in all calculations. Case weights were based on their volume times a density of 0.283 pounds per cubic inch. Propellant weight loss of the redesigned case was equal to the volume displaced times a propellant density of 0.064 pounds per cubic inch. Figure 8 and figure 9 show a section of the proposed redesigned SRB joint and the existing design, respectively. Figure 10 shows an overlay of the two designs. Table 4 summarizes the weight of the two designs. Each SRB contains eight clevis-tang joints, three

of which are termed "field" joints. If a decision is made to incorporate this redesigned joint, all eight joints would be candidates for change. The resulting weight gain per SRB in case material would be 7544 pounds (943 lb per joint) including fasteners. The propellant volume loss per joint due to an incursion of the redesign is 15,700 cubic inches. The weight of this lost propellant is 942 pounds per joint, or 7536 pounds per SRB. In order to assess the impact of the combination of weight increase and propellant loss on STS payload weight, a three-degree-of-freedom trajectory simulation was developed for a typical Shuttle flight, with and without wing normal force constraints, from lift-off to main engine cut-off. Variations of each of these two baseline cases were analyzed in which the available propellant in the SRB's was reduced by an increment of weight and the structural weight of the SRB's was increased by that same increment of weight. Also, the gross lift-off weight was reduced by the amount of payload reduction. Figure 11 summarizes the results of the cases studied in terms of payload reduction versus the increment of weight transferred from SRB propellant to structural weight.

SUBSYSTEM DESCRIPTIONS

Fasteners

The in-line joint flange fasteners were critical to the design due to the high loads involved. Because of this criticality, it was decided to select units already qualified for use on the STS. Standard Pressed Steel Incorporated 1¼-inch MP35N studs with Inconel 718 nuts were determined to be the best choice.

This fastener combination was extensively tested by NASA-MSFC before incorporation into the STS component inventory and the results are presented in

reference 1. The ultimate tensile strength of the studs is guaranteed (by the vendor) to be in excess of 271,900 pounds. Current STS applications include the hydrogen/oxygen tank interface structure, wheels, aft skirt attachment and drogue chute cover attachment. The fasteners will be preloaded to 70 percent of the ultimate strength. The joint load capability shall be 50 percent greater than the maximum applied load. The conceptual design shows a stud with a nut on each end. This was done to expedite removal in the event a thread was damaged during assembly; however, there is not much difference in the space required between a stud and nuts and a bolt and nut. If the design is adopted by the STS, consideration of a bolt/nut combination may be desirable.

Flange Seals

Since sealing was the problem that precipitated this study, considerable effort was directed toward seals that would not fail when subjected to SRB launch under any conditions. Elastomer and metallic "O" rings and metallic "C" seals were evaluated. A Viton elastomer "O" ring and an Inconel 718 "C" seal were selected as the best combination. Three seal diameters were evaluated (1/4", 3/8", and 1/2") and 3/8" was selected to minimize manufacturing and handling difficulties. The properties of the seals considered are included in table 3. Static sealing, tolerances, assembly, and current applications are discussed below.

It was felt that static face sealing is required for this application. The sealing surfaces (or gap) remain fixed in the face seal as opposed to possible gap changes in the current gland sealing. The "O" ring/"C" seal combination was the only configuration investigated in which the compression loads were low enough to assure that the flanges in the seal area could be clamped together. Other seals

are being investigated that will not require a large preload, e.g., spring teflon seals. Backup sealing is provided by the Inconel 718 "C" ring. The rationale for this choice is that if the Viton "O" ring experiences a failure, the escaping gases will be very hot and concentrated, so another Viton ring (600°F melting temperature) may not be effective. The "C" ring can operate continuously at 1800°F and at intermittent temperatures to 3000°F.

The seal integrity can be verified by pressure testing through flange ports in much the same manner as the clevis-tang design. The test procedure must be designed to prevent two anomalies:

(1) A leaking "O" ring must not be masked by the liner seal

(2) The pressurization system must not be capable of damaging the liner or propellant if the "O" ring does leak

A constant volume test system can be designed to satisfy the above requirements.

According to the Parker Seal Co. the most common type of failure of static seals is extrusion of the "O" rings through the clearance gap (table 6). An established design criteria for elastomeric "O" rings at LaRC is that failure is assumed if the ring extrudes into the clearance gap, therefore in-line joint design limits flange deflections (gaps) to very small values. The result of extrusion is nibbling of the "O" ring at the sealing surface and is documented in detail in reference 2. Gap deflections presented for the Viton "O" ring are for a SHORE A durometer hardness of 75 $\pm$ 5 corresponding to current STS "O" rings. It is interesting to note that the "C" seal and the "O" rings are almost equally tolerant of flange deflection at room temperature. Tolerance requirements for

both seals are less stringent than currently used on the SRB hardware and surface finish requirements are the same.

Assembly of the "C" ring can be accomplished with four persons. The ring is very resistant to local distortions. An example is the shipment configuration where the ring is deformed 15 percent (or 18") into an elliptical shape. The 12 foot diameter required for this application is relatively small when compared to the 24 foot maximum diameter produced by the vendor. Some field service for small scratches and other minor damage is available. Applications of "C" seals include the Peace Keeper Missile (MX), head cap and fuel rod seals in nuclear reactors and Pratt and Whitney Aerospace jet engines.

External Fairing

In general, it is felt that external heat protection and aerodynamic fairing for the in-line bolted joint concept are not necessary but a design was developed to be available if required (figures 12 and 13). The design consists of foam filler for the pockets containing the nut (or bolt heads) covered by a layer of cork. Installation begins by casting EPLICON 300 foam in the pockets. The forms are removed after the foam has cured and the cork is bonded in place with epoxy adhesive (Hysol EA 934). Future analysis and design effort should be directed toward determining the need for the fairing and other methods of applying it, such as a spray-on foam system.

Liner Seal

The liner seal (figure 3) is composed of three elements: A soft NBR seal compressed by a pair of rigid phenolic-silca rings. The materials function as charring ablators when exposed to the heat of combustion. This design will prevent hot gas from reaching the steel SRB case if ignition occurs at ambient

assembly temperature and allows insignificant leakage to the case if ignition occurs at lower temperatures. Backup thermal protection is provided through the tortuous path to the casing.

The reason for selecting the above concept in lieu of the current NBR/putty design can be seen in figure 14. Figure 14a presents a simplified diagram of a hypothetical NBR liner bonded to a steel case with a non-interference butt joint. The dark lines represent the butt joint configuration if the temperature is reduced approximately 70°F. The dashed lines depict further contraction due to pressure loading after ignition. It can be observed that this configuration would not prevent gases from reaching the SRB case. In comparison, figure 14b indicates that the gap from the proposed design would be very small when exposed to a 70°F temperature drop. The differences in the gap results from the NBR lengths affected by thermal contraction; approximately 86" for the Clevis-Tang Design because the end is free to move at the field joint allowing contraction toward the factory joint. Reduction of the effective length of the proposed design was accomplished by bonding the free end of the NBR liner at the field joint to a rigid phenolic-silica ring that remains in place when subjected to temperature changes. The resulting NBR length with a free end in the proposed design is 3/8-inch.

Considerable effort was expended on concepts that required bonding the NBR joint at assembly, but they were ultimately rejected because verification was not possible. Consideration was also given to modified versions of the Titan II-C compression seal but it was determined that thermal contraction of the NBR would negate the effects of any practical preload. Also, excessive preloading on elastomer material supporting the rocket motor grain is not acceptable because the

compressed material would tend to deform inward (away from the SRB case) and stress the grain. Cracks in a rocket motor grain allow rapid flame penetration (even if tightly compressed) which would cause hot spots on the case if such a crack terminated at the liner.

Consideration of the above stated problems and requirements led to the conclusion that the internal liner seal must be a rigid entity that could seal without exerting extraneous loads into the grain.

Molded phenolic-silica was chosen for the rigid rings because it has been used in the past as a charring ablator on LaRC reentry payloads and is currently in use in the Scout vehicle Algol rocket motor nozzles. Additional design, analysis and testing will be required to select a reliable method to bond the rings to the steel SRB case. The bonding system must be pliable enough to resist prelaunch temperature changes and yet rigid enough to prevent applying stresses to the grain. One system that should be considered is a thin layer of NBR bonded between the steel SRB case and the phenolic-silica ring. Final machining of the rings would be performed after bonding is completed.

Low durometer hardness NBR is the primary candidate for the compression seal but a new compound must be developed that reduces the hardness without the addition of volatiles. Other elastomers must also be considered that are soft and possess thermal properties equivalent to the NBR liner material now in use. It is felt that this system offers significant advantages over the current liner and development would not entail high risk.

Materials

The materials required for the in-line bolted joint are commercially available and all but two are STS qualified. Molded phenolic-silca is not known

to be used on the STS but is used in the Scout Algol rocket motor nozzle. The soft NBR seal will have to be compounded for use in this application. A list of the intended materials follows:

- o Casing - D6AC
- o Stud - MP35N
- o Nut - Inconel 718
- o "O" Ring - Viton
- o "C" Ring - Inconel 718
- o Liner seal - NBR elastomer
- o Liner seal supports - Molded phenolic-silica
- o External filler - EPLICON 300 foam
- o External Fairing - Cork
- o Epoxy Adhesive - Hysol EA-934

Table 7 summarizes structural, thermal and other properties of the primary materials.

THERMAL ANALYSIS

The primary objective of the thermal design is preventing excessive temperature at the seals. Heat transfer analyses were performed for cases with and without gaps in the insulation. Of secondary concern was heat transfer to the outside of the joint from aerodynamic heating. Because the design for the outside of the joint is similar to the existing (51L) design, the temperature history is expected to be the same as that predicted by Thiokol. These temperature predictions indicate that aerodynamic heating is not a problem.

A transient temperature distribution in the joint during motor firing was calculated for two configurations. In the first case, the insulation was assumed to be sealed at the interface. No hot gases would be allowed to reach the flange seals. The second case assumes a 1/10-inch wide gap at the insulation interface.

Unsteadiness in the flow and the acoustic pressure oscillations were assumed to cause hot gas mixing in the gap, providing a mechanism for hot gases to reach the seals. Only half of the actual thickness of the insulation was included in the models, allowing for possible degradation of the lining during firing. Cork insulation was assumed at the exterior of the joint.

A coarse overall thermal model of the joint (figure 15) was used to calculate the temperature distribution for the sealed insulation case. The calculations were performed using a lumped parameter, finite difference code (MITAS-II). The solution routine was a transient, implicit forward-backward differencing algorithm. Results show that after two minutes of firing, the maximum temperature on the case is 150°F. This is well within the limits of the structure and seals.

For the open gap case, the following approach was used to approximate gas mixing in the gap. The assumption was made that there is no circumferential flow in the gap. Because the gas mixing is expected to take place primarily near the gap opening, an exponential variation of mixing velocity versus path length into the gap was assumed. The equation $V = A \exp(-Bx)$ was used, for which the constants were evaluated at the gap and a point 1/2-inch into the gap. The gap entrance velocity is 150 ft/sec. which was derived from using an experimental SRB Δ pressure of 2 PSI. A compression velocity at the point 1/2-inch inside the gap was calculated for the volume change of the gas due to the pressure oscillations. Cases were run for the 1/2-inch depth velocity being 10 and 100 times this

compression velocity. The gas temperature results versus path length for these cases are shown in figure 16. For both cases, the temperature of the gas in the gap at depths greater than 1.25 inches is not influenced by the mixing velocities assumed at the gap entrance, but is dominated by conduction. These results are felt to be conservative and appear consistent with data generated by Thiokol (Thiokol seventy pound motor test #TS001A, 5-3-86), but are obviously only a first approximation to a very complex problem.

A detailed finite difference model of the flange and the seals in the vicinity of the gap was used to determine temperatures for the above case (figure 17). The insulation is assumed to have a 1/10-inch gap with a path length of 1.5-inch. Because the phenolic-silica insert is rigid, it is felt that any possible gap openings can be held within this tolerance. The maximum temperature on the face of the joint is 301°F (figure 18). The maximum temperature at the seal is 275 °F. These temperatures occur after 120 seconds of firing.

The possibility of developing a leak cavity between the liner seal and "O" ring seal during firing was not considered in the thermal analysis. The insulation was assumed to have either a perfect seal or gaps existing from the time of ignition. If a leak develops through the insulation during firing, hot gases will flow until the pressure on both sides of the insulation is equal. In the joint design, the volume of gas between the insulation and seals is minimized. This, in turn, minimizes the time it would take for the pressure to equalize in such an event. It is expected that the pressure would equalize and hot gases cease to flow before damage to the seals could result.

In summary, the thermal analysis shows that the joint remains at very low temperatures throughout SRB firing if hot gases are prevented from reaching the seals. If a gap in the insulation is present, the mixing of hot gases into that gap occurs primarily near the opening. The stagnant gas in the remainder of the gap acts as insulation. Thus, the joint may still be kept at low temperatures by providing a long path length through the insulation.

STRUCTURAL ANALYSIS

Included in this section is a description and the results of the design model used to develop the basic in-line bolted joint concept, and a description and summary of a detailed finite-element analysis of this concept.

The key to this concept being effective in sealing the joint is the inward offset of the studs from the casing wall. With the centerline of the studs being located radially inward of the casing's mid-surface, a moment (a couple is created by the casing's axial load and the bolt load) is induced which tends to rotate the flange so as to close or seal the joint. This moment more than counteracts the pressure loadings which tend to open the joint. For the usual bolted exterior flange design, the axial load, as well as the pressure load, tend to open the joint in the seal region. However, by locating the studs inboard, the axial load can be utilized to actually close the joint.

Simplified Model

In order to perform the preliminary sizing of an alternate SRB joint, a two-dimensional simplified joint model was developed to evaluate four bolt sizes (1.00", 1.125", 1.25", 1.375") and to determine the number of bolts needed. Design constraints considered were:

- o External loads (see loads section, page 8)
  - 18 million pounds axial force (T_o)
  - 1000 psi internal pressure (p)
- o Bolt and nut parameters
  - strength
  - geometry
- o Casing geometry
  - 146.1" outside diameter (R_o = 73.05")
  - 0.479" shell thickness (t = 0.479")

The two-dimensional joint design model (figure 19), was developed to assess the force and moment equilibrium of a one-bolt segment of the joint by considering: the external shell loads, bolt preload, and location and resultant of the bearing force resultant load. Because of the two-dimensional nature of the model, equilibrium was necessary only in the axial direction. The forces around the circumferential direction were assumed, for design purposes, to uncouple from the axial direction. By fixing the outside radius and thickness of the casing and working with the nut geometry (table 8) for the four bolt sizes, the center of the bolt, R_b and inside radius, R_i, can be determined (table 9). The results of this model defined the joint configuration.

The pressure shell loads are calculated by assuming that the shell is completely fixed at one boundary ($z = \bar{z}$). Since the joint is not rigid, only fifty percent of the resulting reaction was assumed to be applied at $z = \bar{z}$ (equal to 4.5 times the nut height) as shown on figure 19. These loads are summarized in table 10.

The minimum number of bolts required for a joint concept was determined by assuming that each bolt was preloaded to 70 percent of the ultimate strength and

exactly balanced the applied axial load T_o. To give a margin of safety, the total number of bolts required was taken to be 1.5 times the minimum number required to balance the axial load T_o. This means that each bolt will preloaded to a value approximately 50 percent greater than the expected applied axial load per bolt. Table 11 is a summary of the number of bolts required for each of the bolt sizes considered.

Having determined the number of bolts and the magnitude and location of the design loads, the free-body diagram, figure 19, can be used to determine the centroid of the bearing reaction. It is assumed that the pressure load p is taken out by the circumferential stiffness of the shell and flange. Also, the axial component of pressure load is assumed to be negligible.

Axial force equilibrium for a segment yields

$$F_r = P_1 - T \tag{1}$$

where Fr is the bearing reaction, P_1 is the bolt preload, and T is the applied axial load per bolt.

Moment equilibrium about the center of the bolt at the interface for a segment yields

$$a = \frac{T\,(R_o - t/2 - R_b) - Q\,z - M}{(P_1 - T)} \tag{2}$$

In the above formula, the quantity "a" is the location of the center of the bearing reaction (see figure 19), R_o is the outside radius of casing, t is the casing's wall thickness, R_b is the radius of the bolt centerline, and Q and M are the shear and moment, respectively, acting at z = z.

The loads Q, M, and T (see figure 19) that are used in equations (1) and (2) are the forces and moments per segment based on the spacing indicated in table 11. In order for the joint to maintain compression, the bearing reaction in equation (1) must be positive, since the interface can not support a tensile reaction.

Also, it is preferred that the location, a, of the bearing reaction, F_r, be positive (toward the centerline) to ensure that the joint is in compression in the seal region. Table 12 summarizes the location and magnitude of the bearing reaction for the four bolt sizes considered. The larger the value of "a", the closer the center of the bearing reaction will be to the O-ring seal region.

Other geometry considerations are the weight and web thickness. The joint weight can be estimated by approximating the joint segments as simple shapes, computing volumes, and using a weight density of 0.283 lb/in^3. These weight estimates are not intended to be exact but are only to be used to assess one design against the other. The nominal web thickness is estimated by computing the mean chord length of a segment and subtracting out one nut diameter and .32" for fillets. For web stress calculations, the web area is then approximated by multiplying the web thickness by one nut diameter. This area is used to stiffen the joint and transmit the axial load across the joint. The results of the weight and web area calculations are given in table 13. The table shows the web areas to be insufficient for bolt diameters of 1.00" and 1.125".

This design study indicates that a good design candidate would be 144-1.25" bolts, which is the design analyzed in detail in the next section. This conclusion was reached since the 1.25" bolt design weighs less than the 1.375" bolt design (by comparison, 18 percent less) and the net bearing reaction is larger than for the other bolt designs.

Finite-Element Analysis

The approximate analysis using the simplified model of figure 19 led to a configuration for further study using the finite-element approach. This section presents and discusses the finite-element model, the boundary conditions, applied loadings, stresses, and joint opening.

Model Description. - In order to assess the response of the joint to the applied loading, the finite-element model shown in figure 20 was developed. To take maximum advantage of symmetry, a 1.25 degree wedge was used (about 1.59 inches of arc), which represents exactly 1/2 of a bolted segment. In the vertical direction, a 28-inch long segment of the joint region beginning at the flange interface was modeled. The 28-inch vertical height was chosen so that the top of the model was sufficiently far from the flange to not be influenced by the presence of the joint boundary conditions.

The primary components of the model are the shell, web, flange, and the bolt and nut assembly. A summary of model's features is given below:

- o 524 nodes
- o 3 translational degrees of freedom per node
- o 348 elements consisting of:
  - 220 eight-node brick elements
  - 44 six-node wedge elements
  - 84 four-node membrane elements

Boundary Conditions. - Boundary conditions used in the analysis are shown in figure 20. Symmetry conditions were imposed on both the zero degree and the 1.25- degree faces such that no displacement could occur in the circumferential direction at these nodes. The bolt nodes at the flange interface were constrained in the axial direction.

Since nodes at the flange interface must be free to lift off the contact surface but are constrained in the opposite (bearing) direction due to symmetry, an iterative approach was utilized to insure this condition was met. Nodes at the interface had to be capable of supporting bearing loads, but could not

resist tensile forces. To achieve this requirement for a given load case, finite-element runs were repeated with axial boundary conditions at the interface systematically changed until only compressive reactions existed and nodes not in compression were free to lift off of the contact surface.

Applied Loads. - A 204,400 lb preload, as discussed in the last section, was applied to the bolt. The preload was input into the model by enforcing an initial strain condition on the shank section of the bolt. This preload was verified by summing reactions of the bolt nodes at the flange interface, in the absence of all other loadings.

After a converged solution for the SRB ignition load case was effected, the bolt reactions were integrated and found to be 176,300 lb, which is approximately a 14 percent reduction in the applied preload. This finding appeared to contradict an expected increase in the applied preload. Further evaluation of the finite-element displacement results revealed that this bolt unloading phenomenon was due to a Poisson effect that thinned the flange as it was displaced outward in the radial direction; this effect is shown in figure 21. The far right vertical line should represent the equilibrium position for the bolt-flange coupled stiffness under a fixed applied axial load (neglecting any Poisson effects). For this case, the bolt load does increase above the preloaded value. However, since the flange is displaced out radially, which causes a .002" thinning, the flange stiffness curve is shifted to the left the same amount which does result in the 14 percent reduction in the bolt load due to the strain reduction in the bolt.

The external loads (see loads section, page 8) applied to the model were as follows:

Internal Pressure: 1000 psi

Axial Load: 18×10^6 lb

The axial load includes the effect of a bending moment of 95.1×10^6 in-lb. The load, T_b, attributed to the bending moment was taken to be the load resulting from the bending stress if it were uniform around the entire circumference, i.e.,

$$T_b = (M\ R/I)\ (2\pi R\ t) = 2\ M/R = 2.6 \times 10^6 \text{ lb}$$

where: M = bending moment

R = radius of cylinder

t = wall thickness

I = cross-section moment of inertia

It is noted that combining the axial load associated with the pressure of 1000 psi with the above load of 2.6×10^6 lb does give a total load in excess of 18.0×10^6 lb. However, reference 1 states that the maximum combined axial load (including the bending moment effect) for any joint at any time is 17.8×10^6 lb. This apparent discrepancy is thought to be due to the reference including a compressive loading due to thrust. Hence, a total equivalent axial load of 18×10^6 lb was chosen for the finite-element analysis.

The axial load was applied to the model as an equivalent axial stress of 81,609 psi (i.e., 18×10^6 lbs/$2\pi Rt$). As stated in the load section on page 8, the worst case from a stress standpoint was chosen for documentation. However, there are load cases that can result in a larger gap at the inside edge of flange. Limits on the gap due to these load cases are discussed in the results section.

In addition to the internal pressure and axial loads, a vertical force, due to the seals, of 500 lb/in was applied across the inside edge of the flange interface by applying an equivalent pressure on the inner row of elements on the flange bottom.

All pressure and stress loads were applied to the model as element pressures acting on four-node membrane elements overlayed on the appropriate solid elements. A graphic representation of the loads is displayed in figure 22.

Model Verification.- As a means of verifying the finite element model, displacement and stress results in the far-field region of the model were compared with classical thin-shell theory. These results are summarized in table 14.

Results.- Results of the finite-elements analysis are presented below, and include the following:

- o deformed geometry
- o displacement contours (footprint) of the flange
- o nodal axial stress contours
- o nodal circumferential stress contours

Figure 23 shows the exaggerated deformation of the model under the applied loading. Radial displacements are as follows:

- o 0.314 inches at the top of the model
- o 0.308 inches at the flange interface
- o 0.156 inches at a height of 11.66 inches above the flange interface

Figure 24 shows the vertical displacement pattern on the bottom of the flange. The maximum displacement on the inside edge of the flange interface is 0.0010 inch which represents a 0.0020 inch total gap. The maximum displacement

on the outside edge of the flange is 0.0044 inch, representing a total gap of 0.0088 inch.

While the loading condition analyzed in this report produces the highest stresses it does not necessarily produce the largest inside edge gap. Therefore, an attempt was made to establish reasonable limits for the gap that would cover all possible loading conditions. In order to do this, maximum ranges on internal pressure and axial force were determined. The maximum expected operating pressure for the SRB is 1000 psi. In general, the axial load consists of the tensile load caused by the internal pressure ($P\pi R^2$ type of loading), compressive loading due to thrust, and tensile or compressive loading due to the bending moment. Reference 2 gives the maximum compressive loading due to thrust to be 3.5×10^6 and the maximum bending moment, as noted earlier, from reference 1 is 95.1×10^6 in-lb.

The equivalent axial load, T_b, associated with the bending moment is:

$$T_b = (M\ R/I)\ (2\pi R\ t) = 2\ M/R = \pm\ 2.6 \times 10^6 \text{ lb}$$

Given a pressure and the information above, limits on the axial load at that pressure can be determined by the following equation:

$$\text{Axial load} = P\pi R^2 - \text{thrust load} \pm \text{bending load}$$

An upper limit on the axial load, at a given pressure, would occur with minimum thrust and the maximum tensile load due to bending, i.e.,

$$\text{Maximum axial load} = P\pi R^2 - 0 + 2.6 \times 10^6 \text{ lb}$$

Similarly, a lower limit on the axial load would occur with maximum thrust and the maximum compressive load due to bending, i.e.,

$$\text{Minimum axial load} = P\pi R^2 - 3.5 \times 10^6 - 2.6 \times 10^6 \text{ lb}$$

These limits define an envelope wherein all loading conditions must fall. Several finite element runs were made to determine the inside edge gap at various boundary points on this envelope using the maximum internal pressure of 1000 psi and also at the pressure corresponding to the maximum Q condition, which is 610 psi.

The results of this analysis showed that the loading which produced the worst gap occurred at the maximum pressure and minimum axial load (1000 psi pressure and 10.6×10^6 lb axial load). Under these conditions the total inside edge gap remained less than 0.0035 inches.

Figure 25 shows contours for the surface nodal stress in the axial direction viewing the outside of the shell. The maximum stress is seen to occur in a localized region of the web. This is primarily due to the portion of the axial shell load being transmitted down the web.

Figure 26 shows the axial nodal stress contours viewing the inside of the shell. The area of maximum stress is in the region of highest bending.

Figures 27 and 28 show two views of the circumferential nodal stress contours. The maximum stress is a stress concentration occurring at the edge of the hole.

It should be emphasized that positive margins of safety exist everywhere except in a few locally concentrated regions. Nodal stress results for these concentrated stress points are summarized in table 15.

Discussion

While the the proposed design attempts to minimize the gap at the flange interface, it does produce some regions with locally high stresses. Throughout the analysis program, parametric studies were performed that suggest these high

stress areas can be tailored to yield acceptable stresses. There does, however, seem to be a consistent trade-off between stress levels and gap size. For example, moving the bolt circle outward reduced the stresses somewhat but resulted in a larger gap. Another model, in which the transition region was lengthened, resulted in significantly reduced stresses, but also created a larger gap. Reduced stresses and gap openings can be achieved by increasing the shell thickness locally, in the region of the highest bending, but at the expense of increasing weight.

Based on the various analysis results, in order to minimize the gap, the shell transition needs to be as sharp as possible so that a larger percentage of the axial load is transmitted down the outer portion of the web. The larger the force transmitted down the outer edge of the web, the smaller the force transmitted down the shell to the inside edge of the flange. This will develop a larger bending moment across the flange, resulting in a tendency to close the gap. By tailoring the thickness of the shell, web, and flange, a model meeting all criteria for stress, gap, and weight should be possible.

It is noted that recent preliminary results from analyses of variations of this design show significant reductions in stresses and essentially zero gap (compression) over the entire O-ring sealing region.

AERODYNAMIC DRAG ANALYSIS

The design of the new field joint does not allow the joint to extend beyond the SRB surface. Thus contribution to the overall drag load will approach zero. The existing SRB field joint includes a step protruding approximately 0.88 inch

into the free stream. The drag load on this existing step during a Shuttle launch was computed by the equation

$$D = \pi [(r + H)^2 - r^2] \quad (P_f - P_b)$$

where r is the SRB radius, H the step height, P_f the face pressure (windward), and P_b the base pressure (leeward).

The face pressure (windward) was computed using empirical data of the pressure at a raised step within a boundary layer referenced to free stream conditions (ref. 6). The base pressure (leeward) was computed from a correlation of the local unit Reynolds number with a characteristic length based on the boundary layer thickness and the step height. Thus the drag on the existing field joint is based on pressure disturbances from a raised step within a boundary layer. For the first field joint step located 50 feet from the leading edge the drag was computed to be 2286 lbf based on a face pressure of 825.3 psfa and a base pressure of 15.28 psfa.

For instance, at the maximum dynamic pressure of 650 psfa, the corresponding free stream conditions were (local conditions were not available):

$M = 1.42$

$P = 458.57$ psfa

$T = 392.1°R$

$\mu = 9.03 \times 10^{-6}$ lbm/ft-sec

$\rho = .021$ lbm/ft^3

$V = 2378.3$ fps

$Re_C = 3.2 \times 10^6$ ft^{-1}

where M was the Mach number, P the pressure, T the temperature, μ the viscosity, ρ the density, V the velocity, and Re_c the Reynold's number per foot. Assuming flat plate analysis, and that the local conditions were equal to the free stream conditions; for the first field joint step of the existing SRB located 50 feet from the leading edge, the face pressure was 825.4 psfa and the base pressure was 15.28 psfa. Therefore, the drag was 2286 lbf where r = 73.071 inches.

MANUFACTURING

The SRB cases are made of D6AC carbon steel and are forged into the segmented configurations required by the design. These forgings contain no welds to assure that the full strength of the material is utilized. After rough machining they are heat treated to a minimum yield strength of 180,000 psi and an ultimate of 195,000 psi. The fracture toughness values ranged from 90 to 100 ksi inch. These forgings are produced by the Ladish Company in Cudahy, Wisconsin. In order to convert from the current clevis-tang configuration on all the SRB segments except the two end closure hemispherical domes, three forging dies must be remade. Each of these dies are made from a 100,000 pound ingot supplied by one of the larger US steel companies. The proposed SRB flanged motor cases can be made from the present size ingots which weigh about 32,000 pounds. A significant amount of retooling and setup is required in order to fabricate the new cases. However, these are parallel efforts and would be accomplished during the same calendar period. One additional machining operation on the case segments would be required to rough machine the pockets in the flanges that join the two segments together. This could be done at the Ladish facility in Cudahy, Wisconsin, or at the prime machining contractor's plant prior to final heat

treatment. An initial forging production of three motor case segments would be made to check the design and manufacturing process.

No changes in the existing heat treatment would be required since the thickness of the rough machined forging segments on the end are no greater than the existing design. Some retooling and re-setup of existing tooling would be required at the finish machining contractor's plant. An internal expanding mandrel would have to be fabricated, some new handling fixtures and a setup to drill the flanges from the ends as opposed to drilling from the sides. Also a large five axis milling machine would be required to machine the pockets in the flanges after final heat treatment.

QUALIFICATION TESTING

A comprehensive qualification test program is needed to assure that possible hidden flaws in the in-line bolted joint design (or any other concept) are identified before flight. A preliminary basis for such a test program was developed. A two-phased approach to testing was determined to be desirable: (1) establishment of criteria and (2) definition of specific tests. The objective, reasons, and phase descriptions are presented below. The objective is to define a series of tests and supporting analysis by which all STS components affected by the SRB field joint redesign are fully qualified for manned flight. The test environment should be such that the SRB imposes no additional constraints to launch. Two reasons stand out to dictate an all encompassing test plan:

- The number of tests will not be large enough to establish a statistical data base.

- All factors and environments cannot be simulated in each test so design integrity during qualification testing is necessary but not sufficient.

The above reasons demand strong interaction between requirements, predictive analysis and sub-scale and full-scale testing to assure that conditions not simulated never become problems. A partial list of Phase I qualification criteria for the redesign follows:

(1) Structural strength with 140% of expected load

(2) Seating prior to ignition

(3) No O-ring damage during assembly

(4) No O-ring errosion

(5) Load sequencing

(6) Redundant sealing

(7) Installation verifiable

(8) Reuse of motor case

(9) Seal must not leak

(10) Retention of sealing during ignition

(11) Allowable initial gap bounds

(12) Allowable final gap bounds

(13) Allowable maximum temperature range at O-rings

(14) Allowable circumferential flow at seal

(15) Functional predictability of joint

Criteria (10) through (15) are to be determined through developmental tests and analysis.

In addition, developmental tests and analyses are required for early determination of redesign qualification prior to committing to full-scale qualification test hardware. The approach to establish the qualification criteria for items 11 - 15 are presented on table 16. A phase II test outline with accompanying objectives and descriptions, is contained in table 17.

ASSEMBLY FIXTURES

Assembly of the SRB case segments will always be a problem due to out-of-roundness of the mating surfaces. This problem will be inherent in any design because of the thinness of the pressure shell and flanges relative to the diameter. Assembly requirements were studied in detail and a solution was developed that will assure safe assembly of the in-line bolted joint concept. This section describes the preliminary design of an assembly fixture to minimize the out-of-roundness of the SRB joint. The fixture, called the SRB joint circularizer, is described along with the assembly process.

Two main guidelines governed the design of the circularizer. The first is that the strongback should deflect on the order of one-tenth that of the SRB shell, and secondly the jacks should be capable of deflecting the SRB shell approximately 1 1/2-inches on the diameter. Figures 29 and 30 show a plan view and section view of the circularizer, respectively. Figure 31 is a drawing of the alignment pins. A description of the SRB joint circularizer components is given below:

The SRB joint circularizer consists of six main components: (1) the segmented strongback, (2) the jack supports, (3) the jacks, (4) the jack ends, (5) the circular template, and (6) the alignment pins. A description of the components is listed below:

1. The segmented strongback consists of twelve sections made of one W12X53 beam and two C12X25 channels welded together to make a box beam. The twelve segments are joined by either welded or flanged joints. At least two opposite joints would be flanged for ease of setup.
2. The jack supports consist of three 1½-inch diameter extra strong pipes welded to a base plate. Twelve of these supports are then bolted to the joints of the strongback.
3. There are three jacks at each of the twelve strongback joints for a total of 36 jacks. Each set of three jacks has a hand pump valved in such a way that the three jacks can be pumped individually or simultaneously.
4. The jack ends consist of an upper and lower section which are tongue and grooved together to slide in the radial direction when the circularizer is assembled. The upper section connects to one jack and has two-inch bearings on each side.
   The lower section connects to two jacks and has an upper and lower hard rubber pad.
5. The circular template is a plate with the outer bottom surface machined to match the lower flange face within the design tolerances. It also has stiffening webs and lifting lugs.
6. The alignment pins are unthreaded studs with a taper at the end to account for any circumferential or radial misalignment of the bolt holes.

The purpose of the assembly process is to assure that the SRB cases are true circles and provide controlled guidance as the cased segments are brought together. The steps necessary to safely accomplish the SRB case assembly are listed below:

(1) Assemble strongback around the SRB and place around joint

(2) Align 2 opposite jacks at the maximum diameter of lower flange segment

(3) Place circular template over face of lower flange

(4) Load opposite jacks until flange face matches the circular template (figure 32)

(5) Remove the circular template and put seals into place

(6) Lower the upper booster segment and adjust alignment pins to match lower segment bolt holes (figure 33)

(7) Load upper jacks until the reference face of the jack meets with the lower flange and slip the joint into place

(8) Insert and pretorque as many flange bolts as possible

(9) Retract the jack and lift the strongback up to the next assembly joint

(10) Insert remaining flange bolts and tighten all nuts to maximum torque

Some considerations for a final design might include computer control of the jack system and an extension of the acting length of the alignment pins.

CONCLUDING REMARKS

A conceptual design of an alternate Shuttle Solid Rocket Booster (SRB) field joint has been developed which meets the objectives for a safe, reliable and analyzable joint. The design that was selected, from various others considered, is an In-Line Bolted Joint concept. This design incorporates two flanged face seals that are seated and preloaded by bolts at installation and remain seated throughout flight. Internal insulation protects the seals from hot gases and the outside of the SRB case joint is protected from aerodynamic heating by a cork covering.

This concept has been shown by analysis to be structurally and thermally satisfactory. The conceptual design contained in this report has not been optimized however, further refinements of the design should show that:

(a) The flange seal gap can be closed completely

(b) All stresses can be reduced to more acceptable levels

(c) Weight can be reduced significantly

Verification testing of the design is straightforward and the manufacturing techniques are within the capabilities of the SRB vendors but will require at least a 12-month impact to the current STS program schedule.

TABLE 1. REDESIGN EVALUATION CRITERIA

*1. INSTALLATION INTEGRITY IS VERIFIABLE

*2. JOINT HAS REDUNDANT SEAL

3. EXISTING HARDWARE IS UTILIZED

4. SEALS ARE PROTECTED FROM HOT GASES

5. SEALS ARE SEATED AT INSTALLATION AND REMAIN SEATED

6. OPENING OF SEAL GAP IS MINIMIZED

7. DESIGN DOES NOT AFFECT REUSABILITY OF JOINT

8. SIZE OF CAVITIES AHEAD OF SEALS IS MINIMIZED

9. POTENTIAL SEAL DAMAGE ON INSTALLATION IS MINIMIZED

10. DESIGN MINIMIZED ADDITIONAL WEIGHT

11. JOINT IS EASILY ASSEMBLED

12. DESIGN IS BASED ON PROVEN CONCEPT

13. JOINT IS ANALYTICALLY PREDICATABLE

*SAFETY REQUIREMENT (MUST MEET)

TABLE 2. RESULTS OF DESIGN MODEL ANALYSIS

FASTENER SIZE	NO. REQUIRED SPACING	COMMENTS
1.000"	232(1.55°)	NOT PRACTICAL
1.125"	180(2.00°)	WEB AREA TOO SMALL
1.250"	144(2.50°)	JOINT WT. 3040 LBS.
1.375"	116(3.10°)	JOINT WT. 3545 LBS.

* CURRENT CONCEPT USES 144-1.25" FASTENERS WITH ULTIMATE STRENGTH 260 KSI

TABLE 3. SEALS

	PRESENT "O" RING	METALLIC "O"-RING	METALLIC C RING
MATERIAL	VITON	INCONEL 718	INCONEL 718
ALLOWABLE TEMPERATURE	-20°F TO 400°F	-425°F TO 1800°F	-425°F TO 1800°F
COATING OR LUBRICANT	GREASE	SILVER	SILVER
ALLOWABLE GAP*	.008"-.013"	.009"-.011"	.013"-.015"
LEAK RATE	10^{-1} $\frac{CC\text{-}He}{SEC}$	10^{-3} $\frac{CC\text{-}He}{SEC}$	10^{-2} $\frac{CC\text{-}He}{SEC}$
PRELOAD	25-50 LBS/IN/SEAL	2500 LBS/IN/SEAL	450/LB/IN/SEAL
SQUEEZE	.058-.080"	.060-.075"	.075-.080"

*3/8 DIAMETER, 1000 PSI

TABLE 4. STRUCTURAL WEIGHT COMPARISON

	STRUCTURAL WEIGHT COMPARISON (POUNDS)		
	51-L DESIGN	SRB INLINE BOLTED JOINT	DIFFERENCE
JOINT	2,195	2,710	515
FASTENER	67	495	428
		TOTAL PER JOINT	943

NOTE:

1. 12" ON EACH SIDE OF CASE SEGMENT JOINT CONSIDERED TO CALCUALTE WEIGHT
2. EACH SRB GAINS 7,544 POUNDS OF STRUCTURAL WEIGHT (8 JOINTS)
3. EACH SRB INLINE BOLTED JOINT DISPLACES 15,700 IN^3 INTERNAL VOLUME OVER THE EXISTING 51-L DESIGN (942 LB.)

TABLE 5. SRB GAS PROPERTIES

TEMPERATURE	6000°F
PRESSURE	1000 PSI
PRANDTL NUMBER	.472
MOLECULAR WEIGHT	28.69
RATIO OF SPECIFIC HEATS	1.14
VISCOSITY	5.385 E-6 LB/IN - SEC AT 6000°F 1.88 E-6 LB/IN - SEC AT ROOM TEMPERATURE
SPECIFIC HEAT AT CONSTANT PRESSURE	.85 BTU/LB - °F AT 6000°F .1 BTU/LB - °F AT ROOM TEMPERATURE
THERMAL CONDUCTIVITY	5.433 BTU/IN - SEC - °F AT 6000°F 2.08 BTU/IN - SEC - °F AT ROOM TEMPERATURE

TABLE 6. ALLOWABLE GAPS

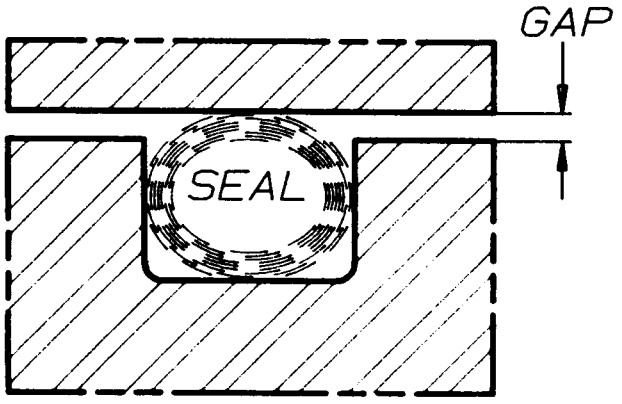

3/8" DIAMETER SEAL TYPE	MAX. GAP ALLOWABLE
METAL "C" RING[A]	.013 - .015
METAL "O" RING[A]	.009 - .011
VITON "O" RING[B]	.008 - .013

A- UNAFFECTED BY TEMPERATURE
B- ROOM TEMPERATURE

TABLE 7. STRUCTURAL MATERIALS

	D6AC	MP35N	INCONEL 718	(1) (2) MOLDED PHENOLIC SILICA	VITON	HYSOL EA934
F_{TU}, PSI	195	273	265	13.5	1915	
F_{TY}, PSI	180	263	215	7.5		
F_{SU}, PSI						3100
E, PSI x 10^{-6}	30	33.9	29.7	1.3	.0008	
K_{IC}, KSI IN	90	78.7	130			
HARDNESS (DUROMETER)					76	

(1) SEE REFERENCES 3, 4, AND 5 FOR FURTHER MATERIAL PROPERTIES

(2) PROPERTIES ARE FROM REF. 3 IN PARALLEL DIRECTION AT ROOM TEMPERATURE

TABLE 8 - NUT GEOMETRY AND BOLT STRENGTH DATA

Bolt Dia (in)	Nut Dia (in) ND	Nut Height (in) NH	Bolt Strength (ksi)
1.000	1.88	1.40	186.0
1.125	2.10	1.57	234.0
1.250	2.36	1.75	292.0
1.375	2.61	1.93	333.9

TABLE 9 - JOINT GEOMETRY DATA

Bolt Dia (in)	R_b (in)	R_i (in)	Flange width R_o-R_i (in)
1.000	72.110	70.532	2.52
1.125	72.000	70.312	2.74
1.250	71.873	70.057	2.99
1.375	71.745	69.802	3.25

TABLE 10 - JOINT DESIGN LOADS

Bolt Dia (in)	z=4.5*NH (in)	Q_o (lbs/in)	M_o (in-lbs/in)	T_o (lbs)
1.000	6.30	2357.0	5553.0	18E6
1.125	7.06	2357.0	5553.0	18E6
1.250	7.88	2357.0	5553.0	18E6
1.375	8.79	2357.0	5553.0	18E6

Q_o and M_o are 50% of the totally fixed reaction

TABLE 11 - REQUIRED JOINT BOLTS

Bolt Dia (in)	Allowable load/bolt (kips) P_1	Minimum Number of Bolts	Required Number of Bolts	Number of Bolts Used (spacing)
1.000	130.2	139	208	232 (1.55°)
1.125	163.8	110	166	180 (2.10°)
1.250	204.4	89	133	144 (2.50°)
1.375	233.7	78	116	116 (3.10°)

TABLE 12 - BEARING REACTION SUMMARY

Bolt dia (in)	a (in)	Fr (lbs)
1.000	0.268	53614.0
1.125	0.386	63800.0
1.250	0.511	79400.0
1.375	0.786	78528.0

TABLE 13 - JOINT WEIGHT ESTIMATES

Bolt dia (in)	Web Area (in^2)	Weight Estimate * (lbs)
1.000	-0.50	2416.0
1.125	+0.22	2814.0
1.250	+1.17	3029.0
1.375	+2.66	3543.0

* weight is based on 24" long segments

Table 14 - MODEL VS. THEORY

DESCRIPTION	THEORY	MODEL
Radial deflection	0.313"	0.314"
Axial stress	81,609 psi	81,692 psi
Circumferential stress	151,505 psi	155,430 psi

TABLE 15 - SUMMARY OF LOCALLY CONCENTRATED STRESS POINTS

	Maximum Nodal Stress[1]	
Model Component	Axial Stress (psi)	Circumferential Stress (psi)
Shell	214,452[2]	175,369
Flange	-159,210	358,860[3]
Web	230,163[4]	85,426

Notes: (1) Based on maximum average nodal stresses

(2) Geometric discontinuity bending stress on the inside of the shell near the transition.

(3) Stress concentration at the edge of the bolt hole.

(4) Concentrated tensile stress on the outer edge of the web.

TABLE 16. ESTABLISHMENT OF QUALIFICATION CRITERIA VIA ANALYSIS AND TEST, ITEMS (11-15)

TASK	APPROACH
(11) Establish allowable initial gap bounds	Predict maximum initial gap based on design tolerances and analysis Verify analytical assumptions via sub-and full-scale assembly tests
(12) Establish allowable O-Ring final gaps for worst case conditons.	Analysis performed to determine preliminary final gap range due to flight loads. O-ring developmental tests performed over this range and over parameter ranges of Pressures, pressure rates, O-ring tolerance lubricants, mechanical properties, pre-launch temperatures and dynamic excitations
(13) Establish max. allowable temperature range at O-rings.	Determined from O-ring material specs, analysis and developmental tests
(14) Establish allowable circumferential flow at seals.	Determined from analysis and fundamental tests
(15) Establish joint functional predictability	Determine via calibrated analysis, time lapse criterion between ignition and resealing. (Could be zero if criterion is retention of seal during ignition.) Determine mechanical behavior characteristics to be used as predictability criteria. Predictability implies calibration of analysis is achievable and valid over a range of loading conditions.

TABLE 17. TEST OBJECTIVE/DESCRIPTION

TEST	OBJECTIVE/DESCRIPTION
A. Sub-scale test	Establish potential of the redesign to meet the structural qualification criteria prior to commitment to fabrication of full-scale test hardware as prescribed by the qualification plan. All features of the redesign should be replicated in the sub-scale model. Loads are appropriately scaled and test instrumentation includes measurements of loads, deflections and strains. Function of joint also assessed and redesign zone of influence and impact of redesign on previously qualified hardware indicated.
B. Assembly tests	Provides necessary understanding of the effect of tolerances on initial gaps and qualifies assembly operatings, jigs and quality assurance procedure to eliminate o-ring damage. Tests are on sub- and full-scale hardware.
C. Hydro tests	Verify joint functional behavior under hydro induced pressure loading and simulated ignition transient. Full-scale tests are required to qualify redesign for final gap criterion as determined from developmental tests. Loads should be taken above limit where possible. Tests with single and/or damaged o-rings permit verification of redundancy criterion.
D. Sub-scale firings	Verify effectiveness of redesign to protect seals from excessive thermal environment and circumferential flow. Sub-scale firings are required to establish meaningful statistical data base. Thorough instrumentation will be necessary to define pressure, temperature and flow. Indicates redesign region of influence.
E. Full-scale firing	Test sequence culiminates in this final qualification test. Full-scale replication is required and vertical orientation is preferred. Full instrumentation is necessary to determine if redesign meets all criteria on final gap range, pressure, temperature, flow and joint function. Where possible, limit loads may be exceeded by margins. This is the only test that qualifies full-scale hardware with full environment set and sequence over established redesign region of influence.

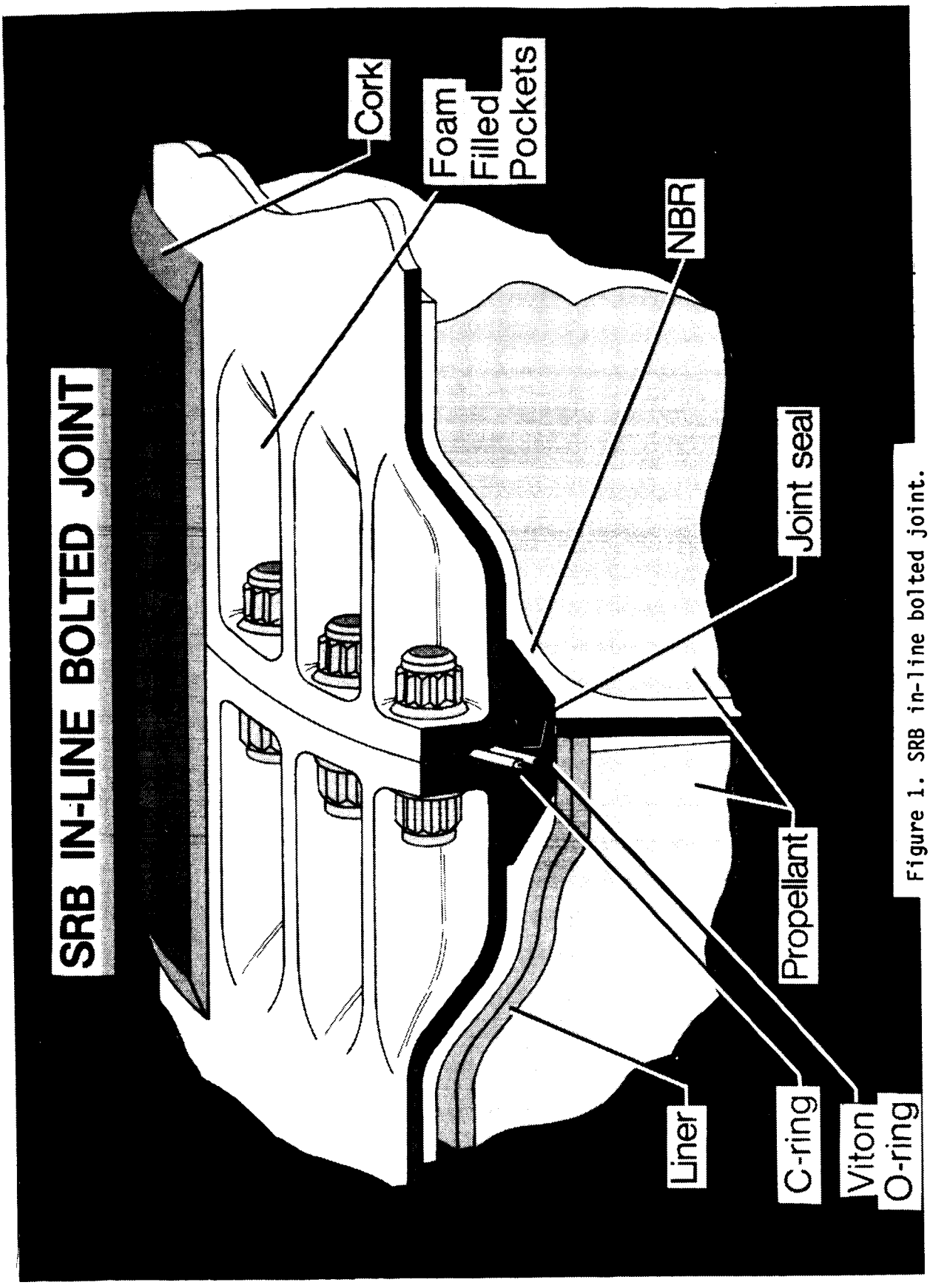

Figure 1. SRB in-line bolted joint.

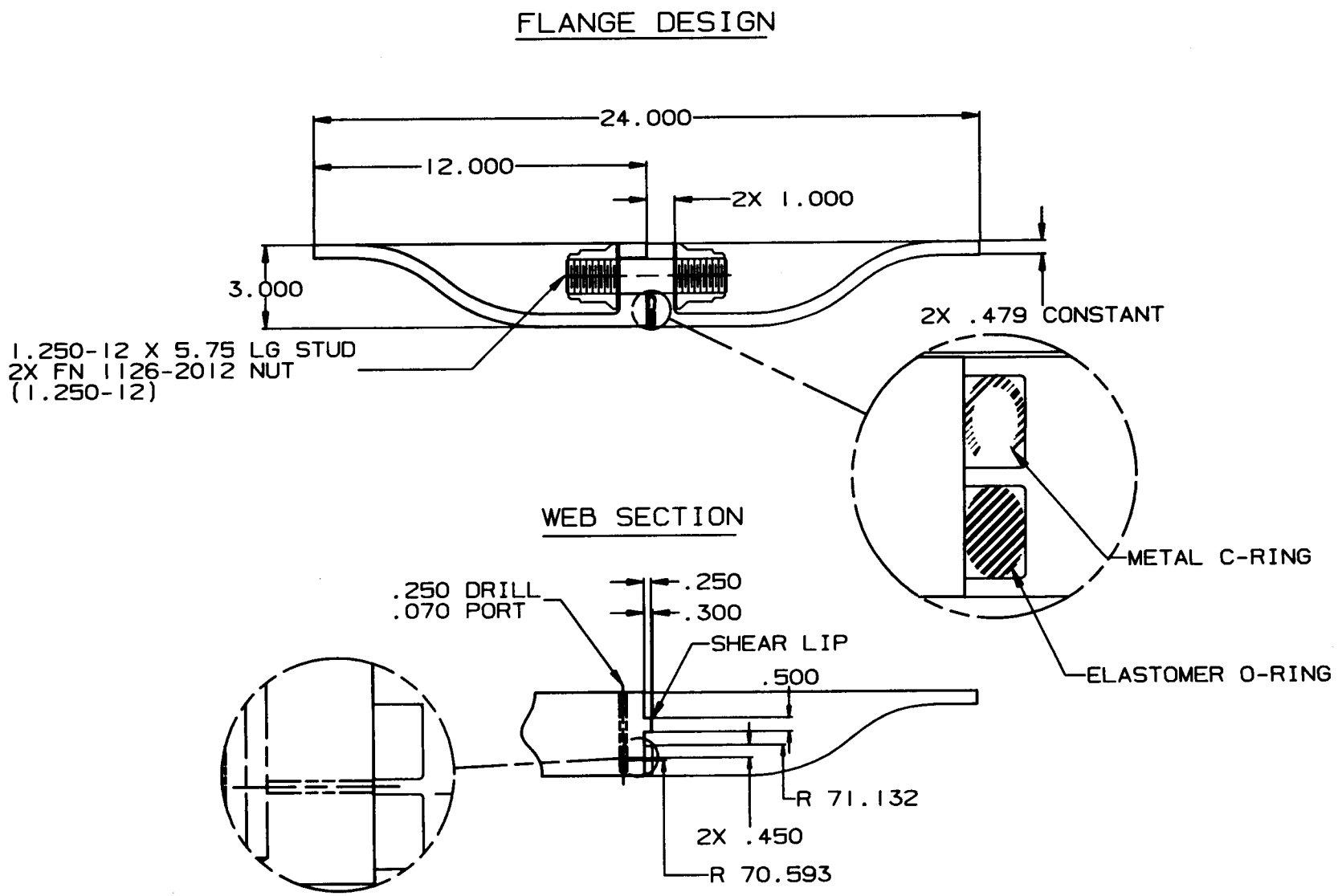

Figure 2. In-line bolted joint flange design.

SRB LINER SEAL CONCEPT

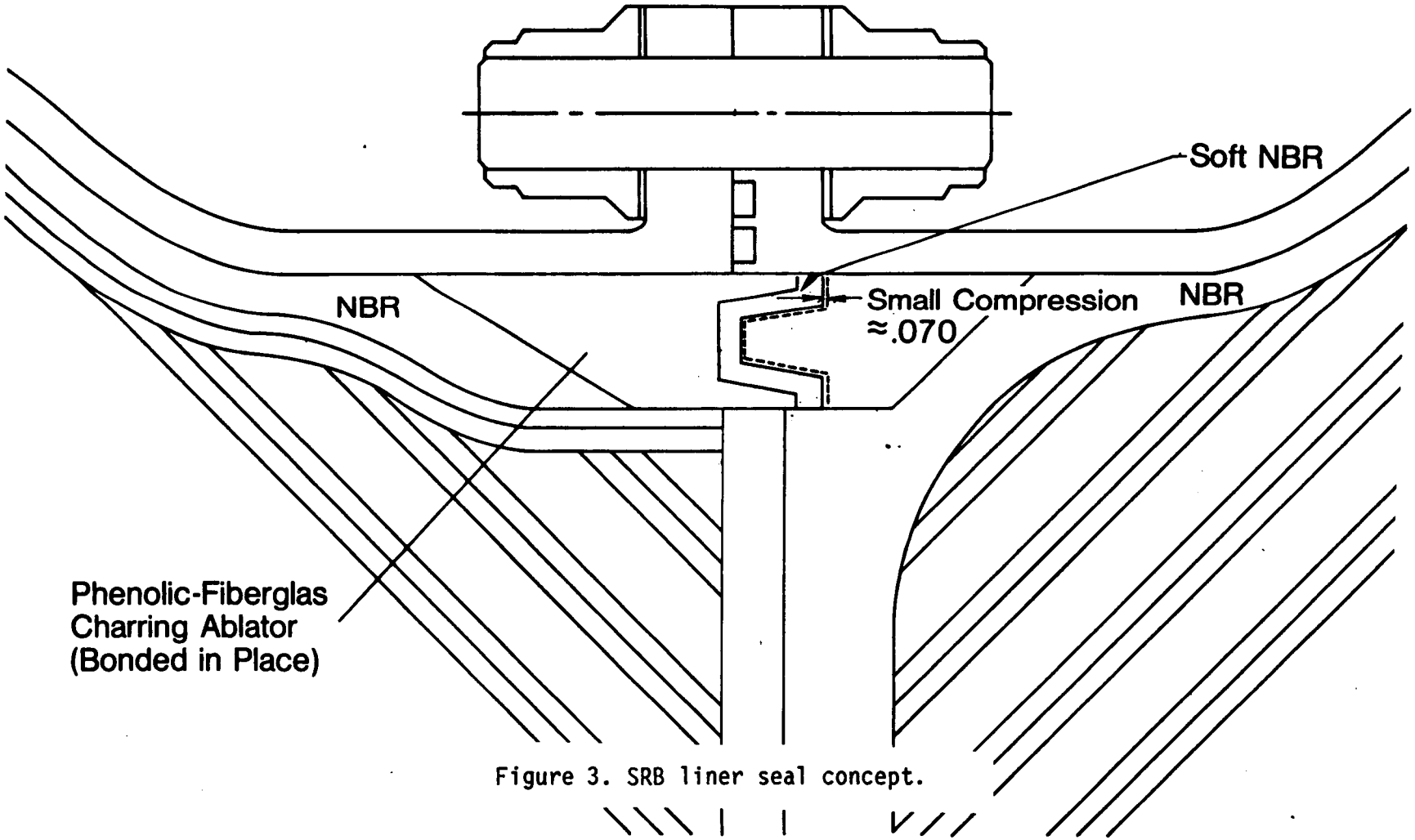

Figure 3. SRB liner seal concept.

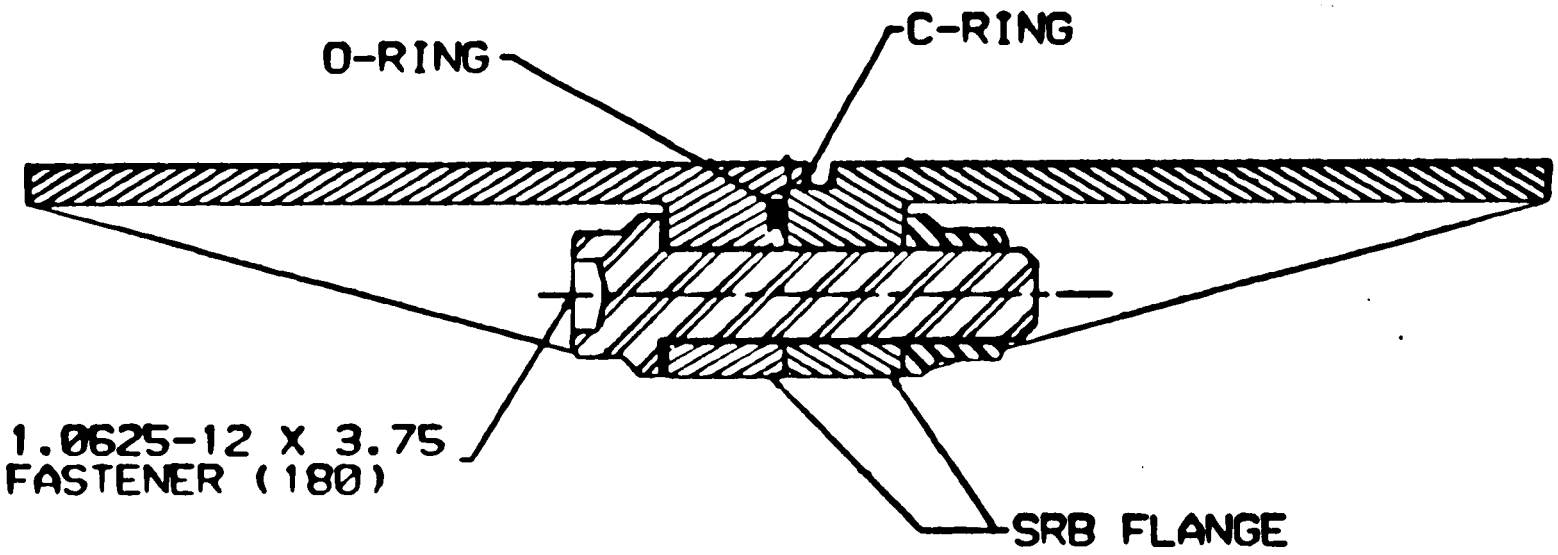

EXTERNAL FLANGE DESIGN

Figure 4. External flange design.

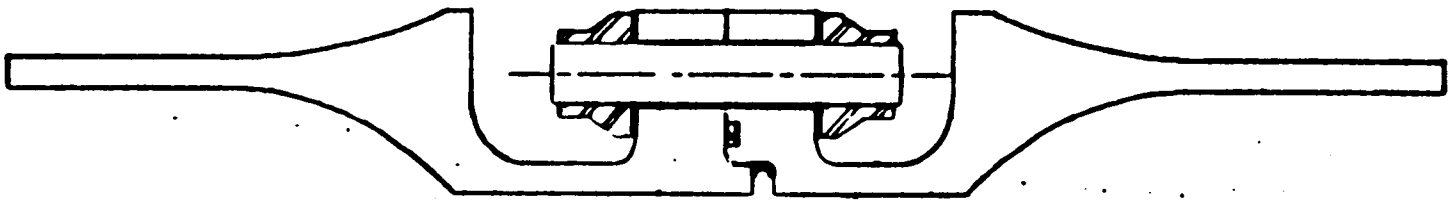

RECESSED FLANGE DESIGN WITH
BOLTS IN-LINE WITH SHELL

Figure 5. Recessed flange design with bolts in-line with shell.

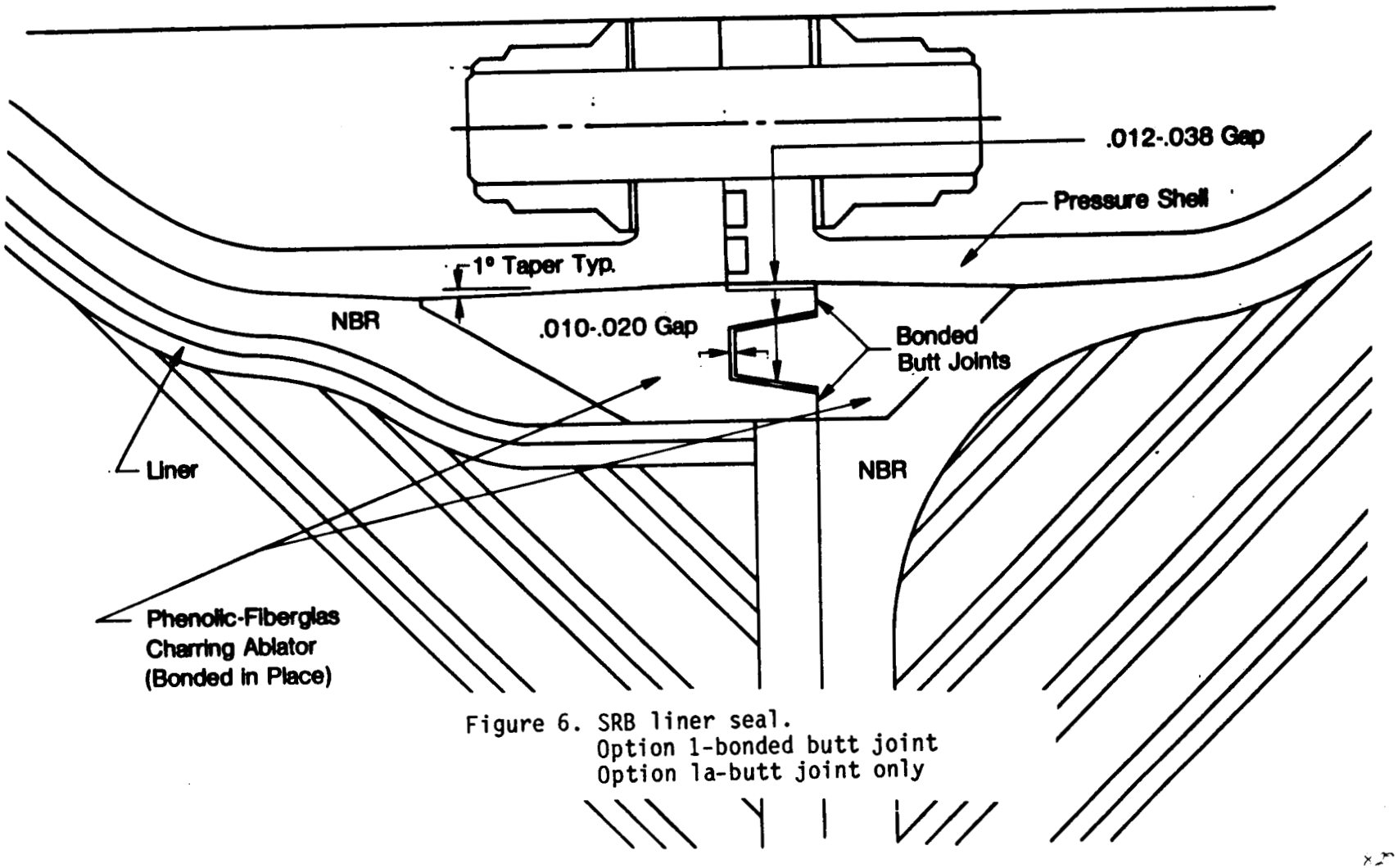

Figure 6. SRB liner seal.
Option 1-bonded butt joint
Option 1a-butt joint only

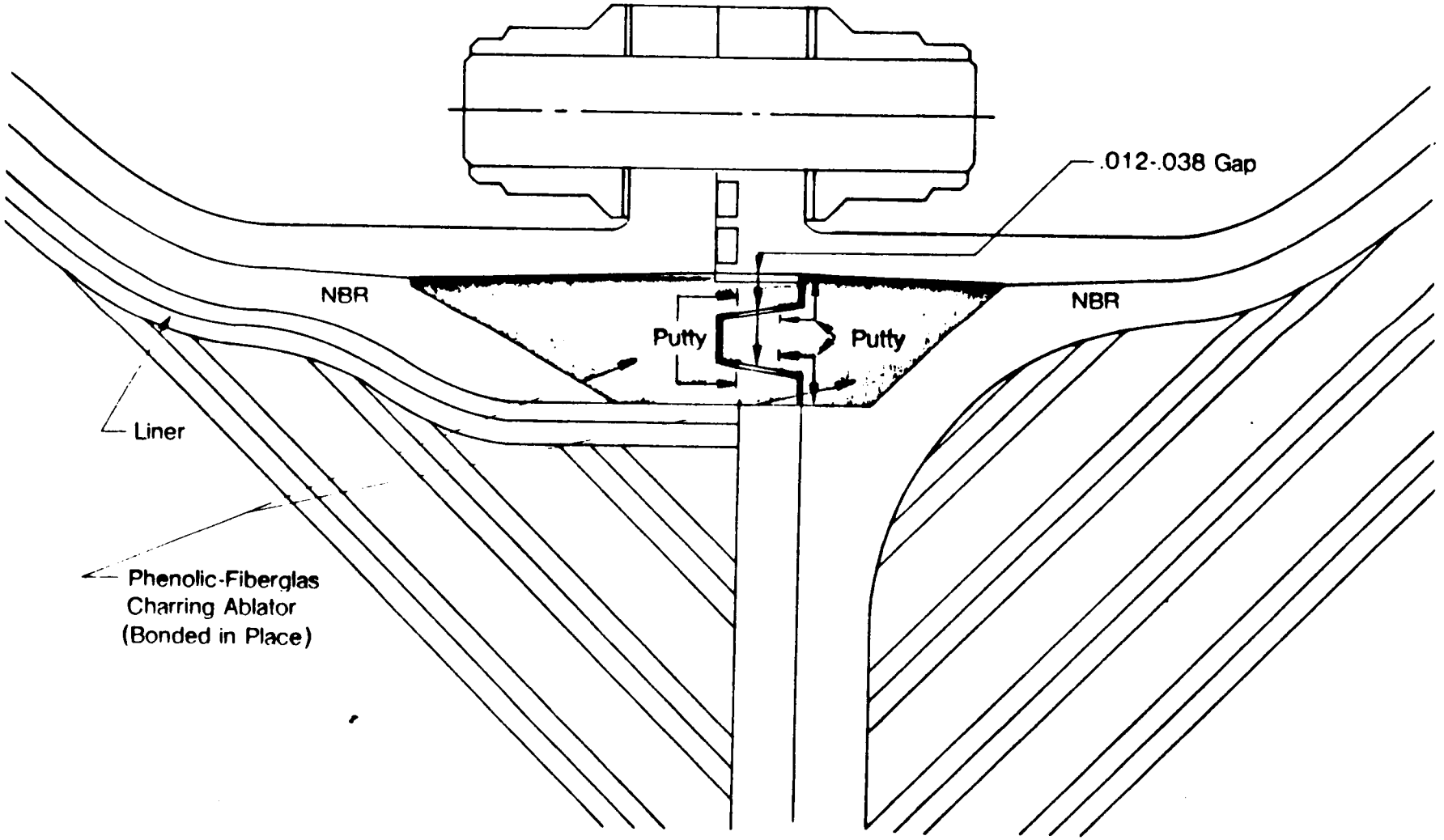

Figure 7. SRB liner seal.

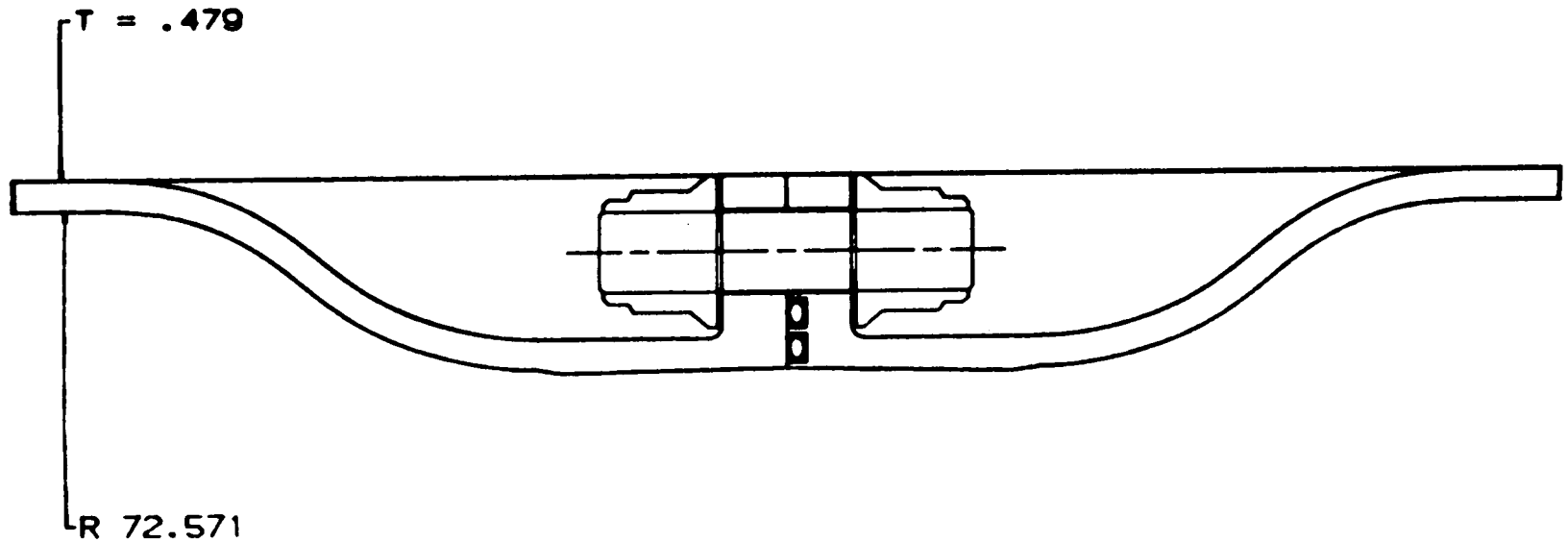

Figure 8. Schematic of proposed LaRC redesigned joint.

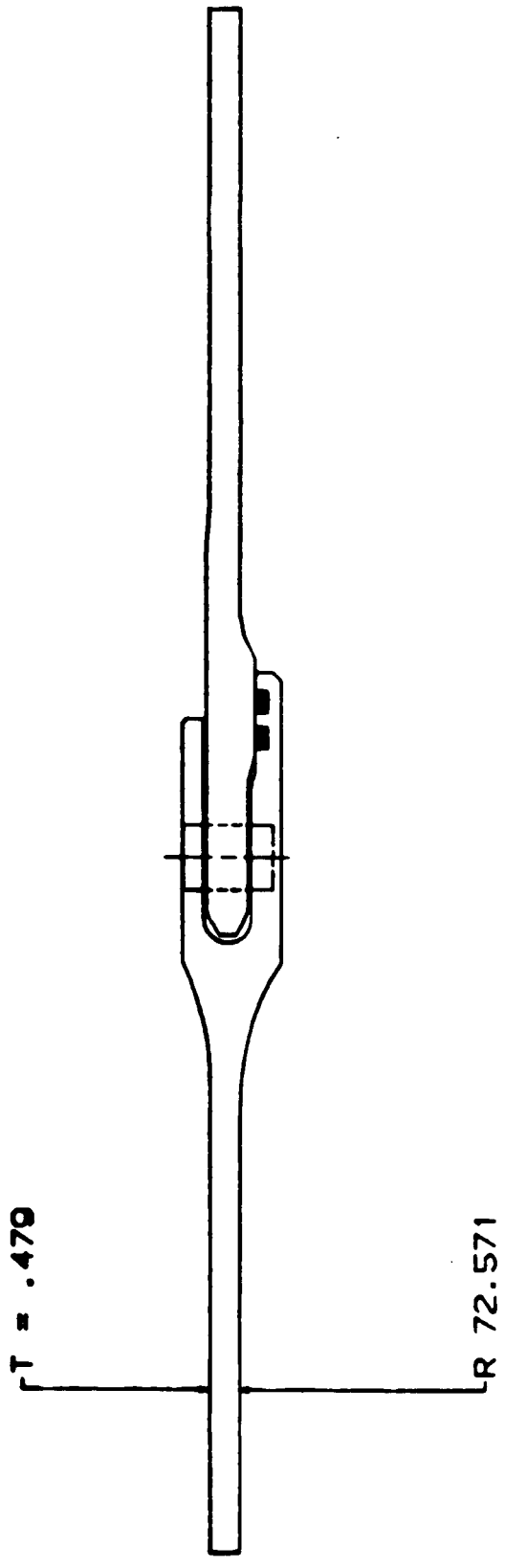

Figure 9. Existing SRB joint design.

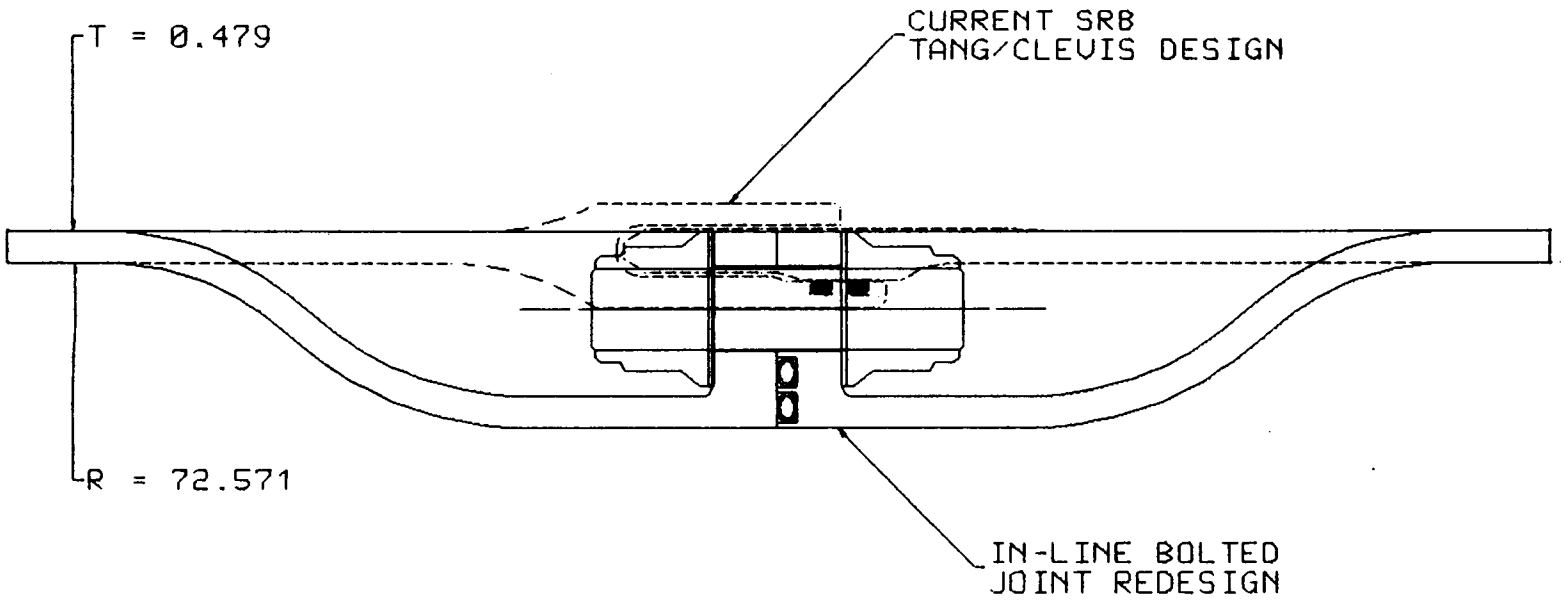

Figure 10. Comparison of proposed LaRC in-line and clevis tang joints.

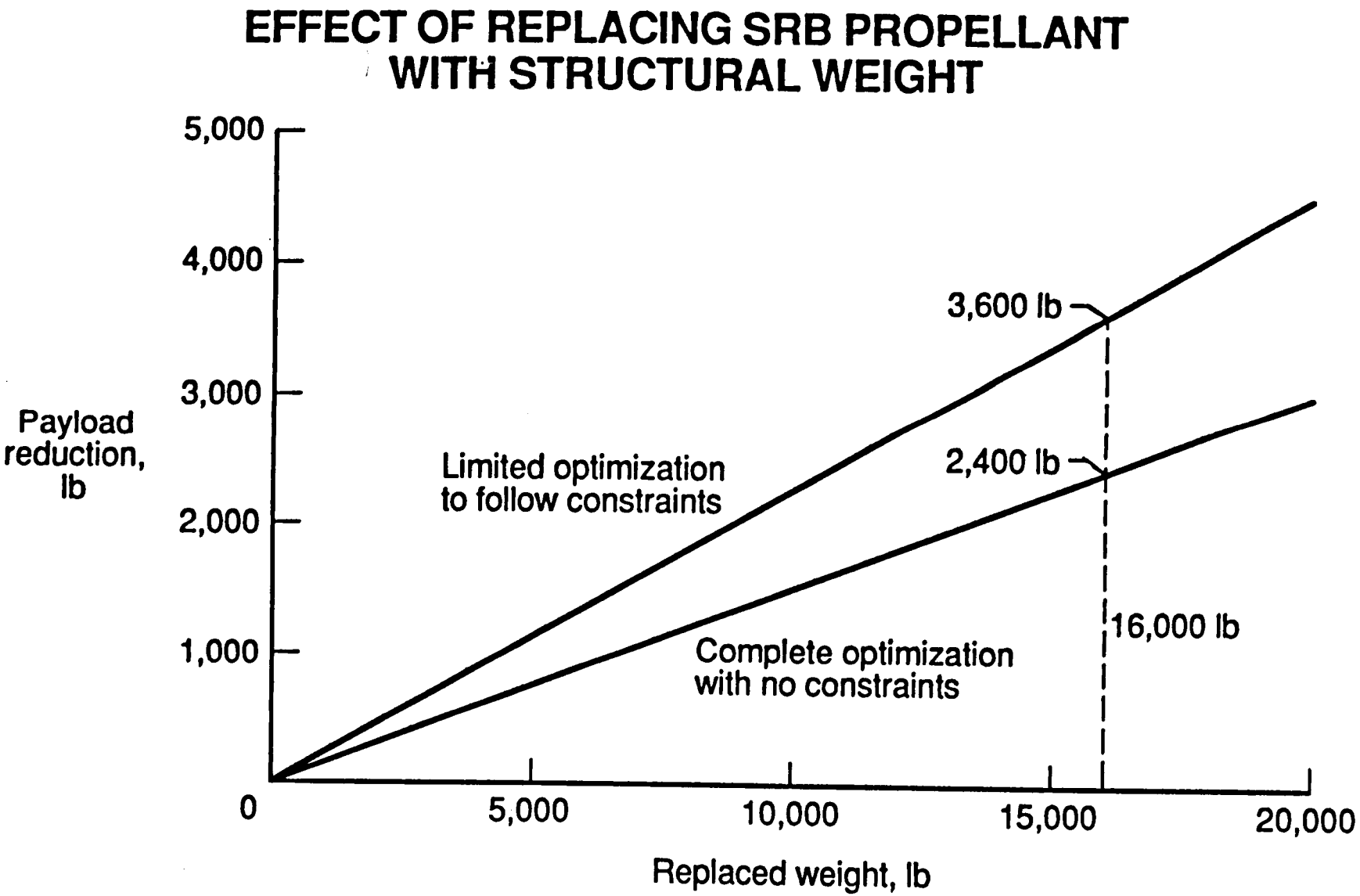

Figure 11. Effect of replacing SRB propellant with structural weight.

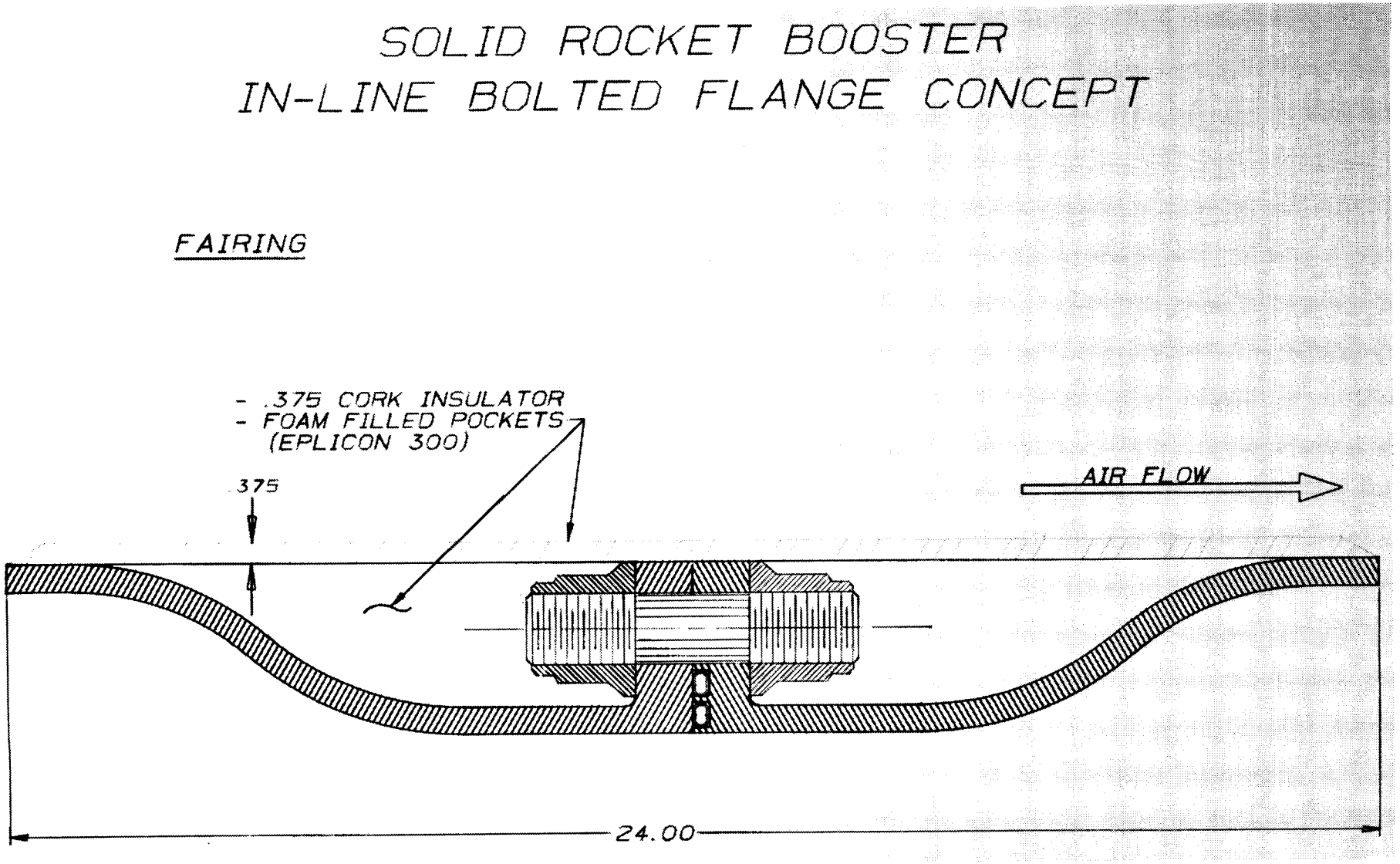

Figure 12. External fairing section view.

SOLID ROCKET BOOSTER
IN-LINE BOLTED FLANGE CONCEPT

FAIRING

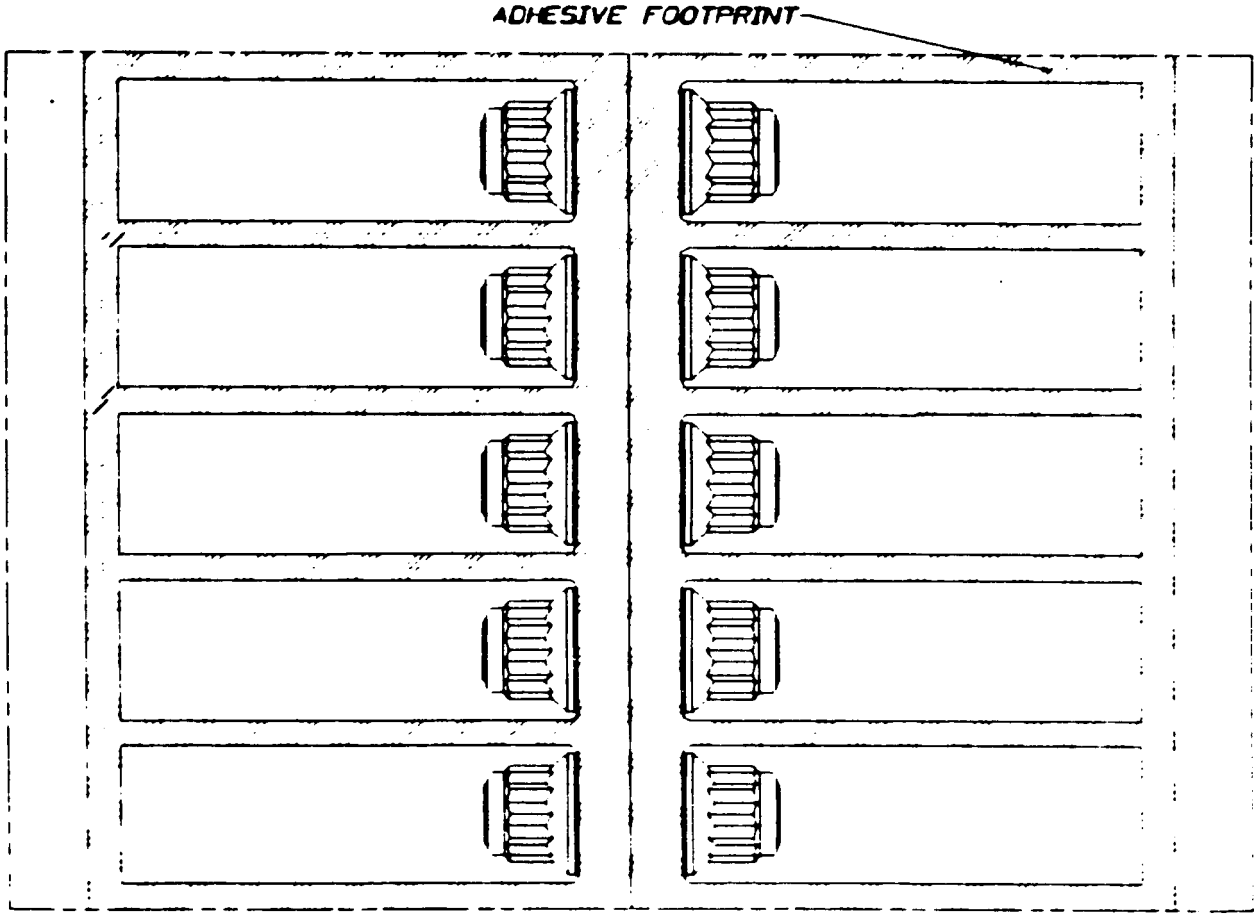

Figure 13. External fairing adhensive footprint.

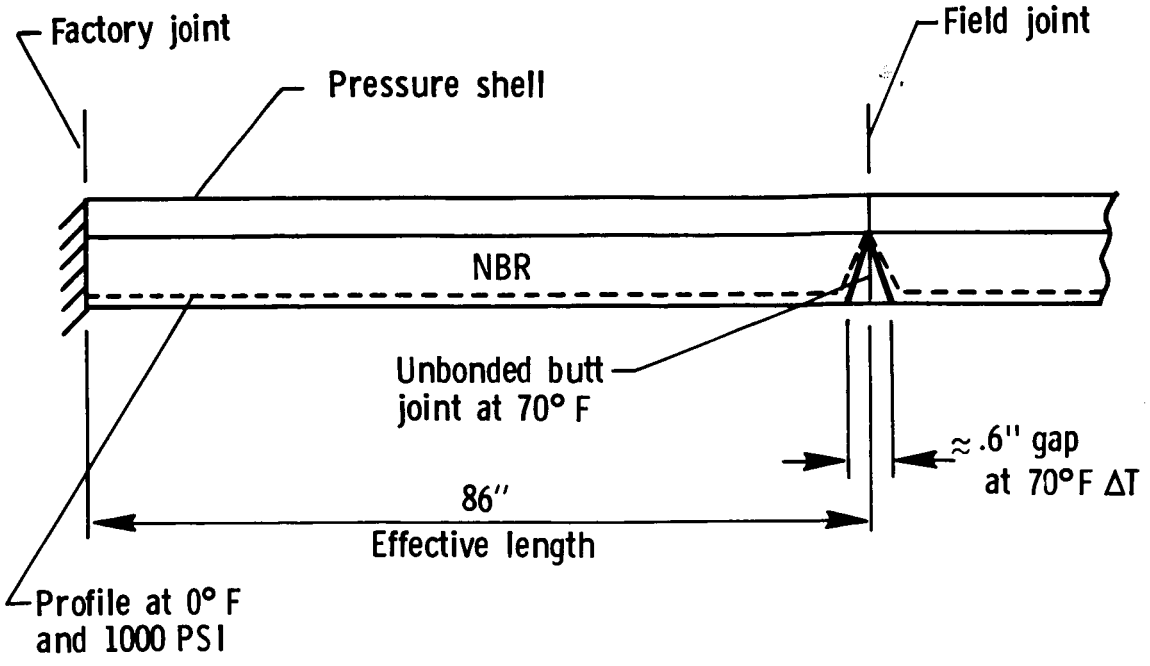

(a) Current design.

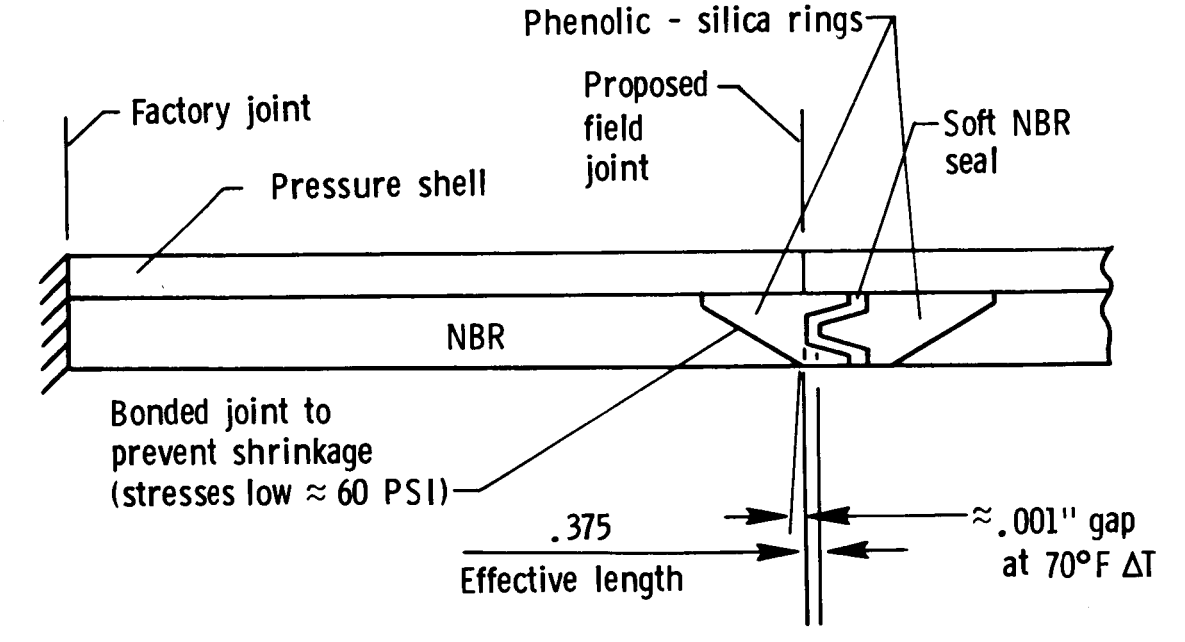

(b) Proposed design.

Figure 14. Schematic of NBR liner shrinkage profile.

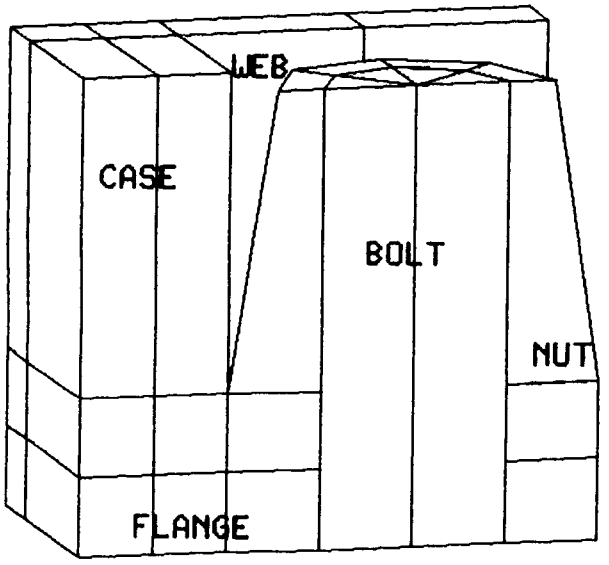

FINITE DIFFERENCE

THERMAL MODEL

TEMPERATURE GRADIENT

(DEG. F)

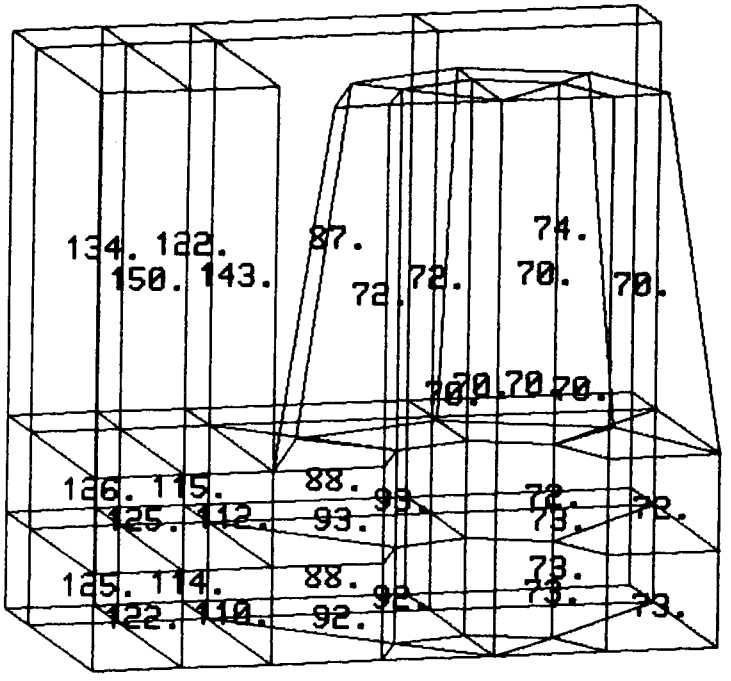

Figure 15. Coarse thermal model.

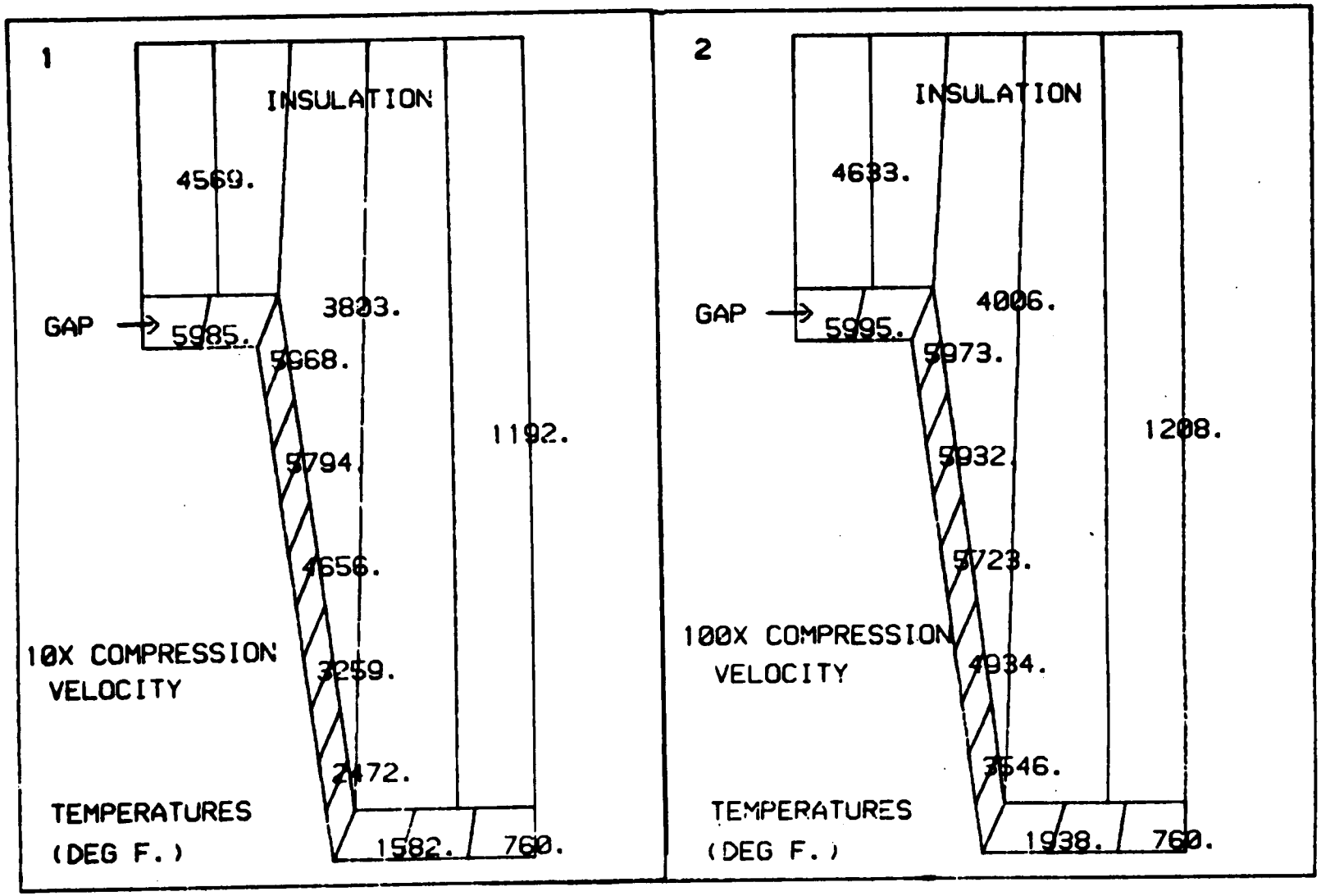

Figure 16. Gap/insulation temperatures.

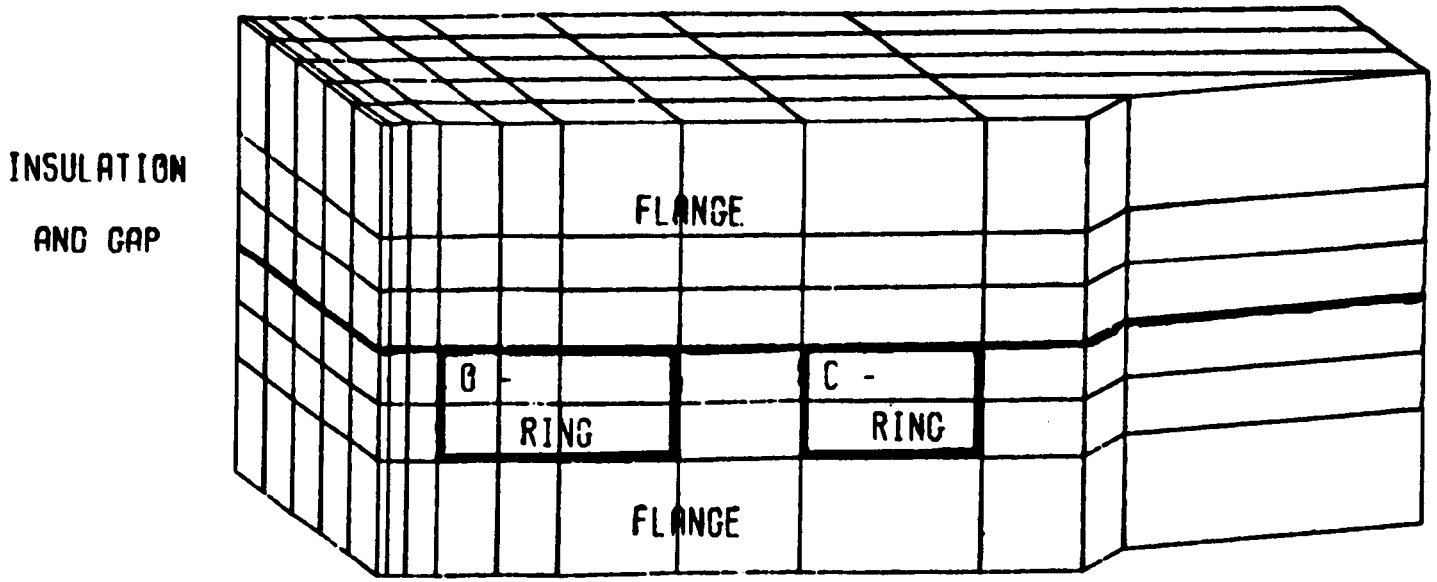

Figure 17. MITAS-II thermal model.

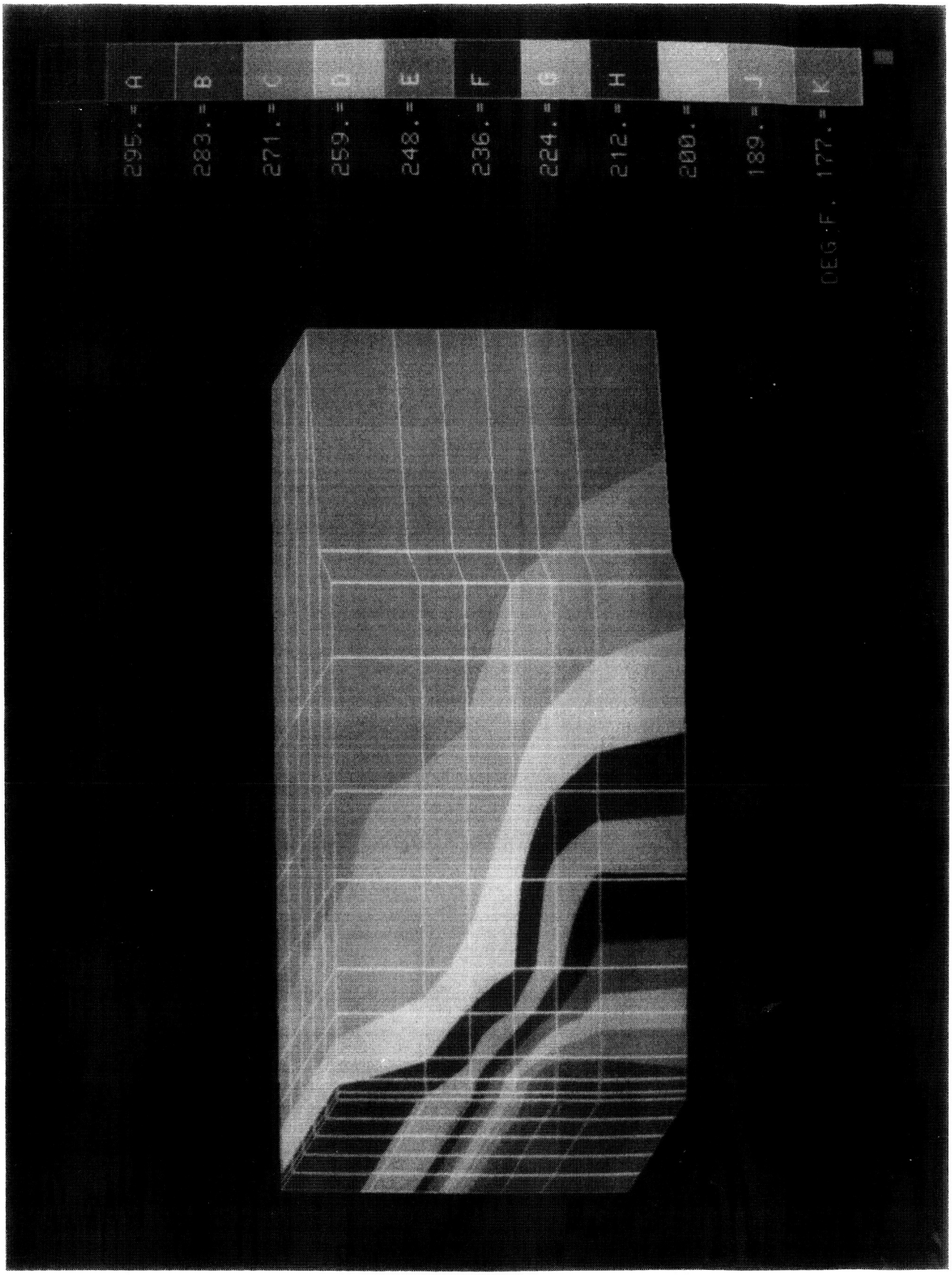

Figure 18. MITAS II temperatures.

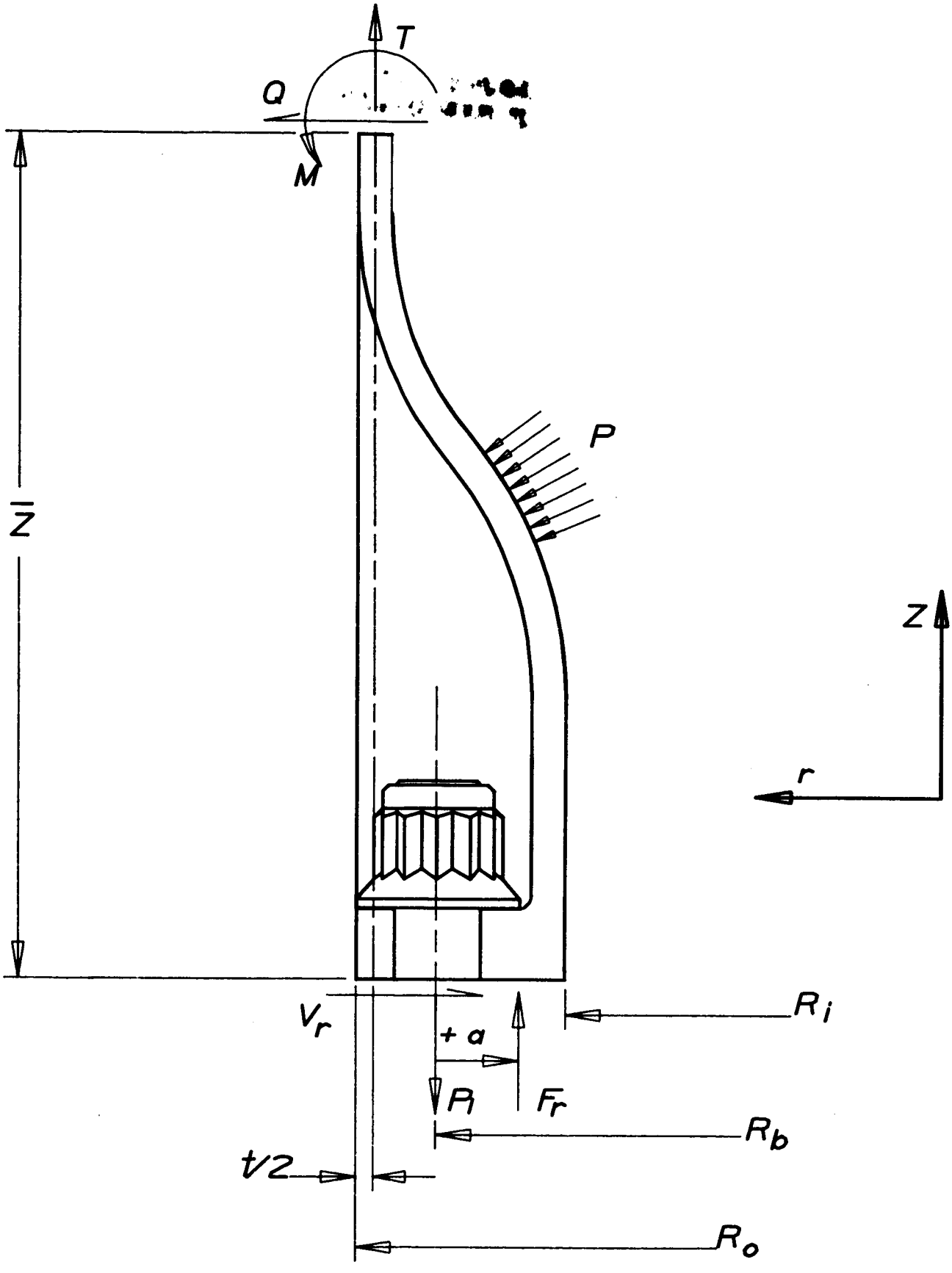

Figure 19. In-line bolted joint concept analysis model.

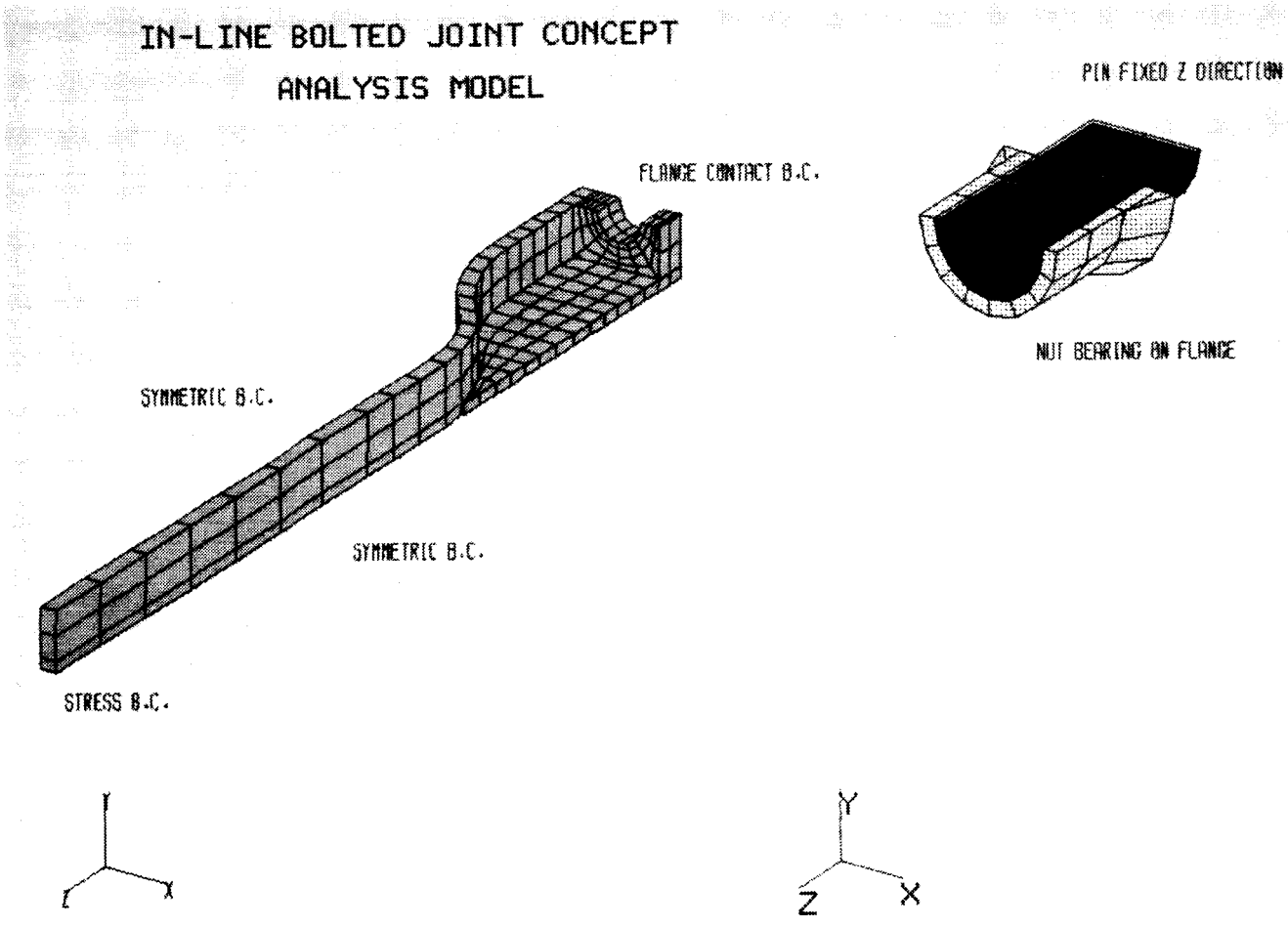

Figure 20. Preloaded bolt finite-element model.

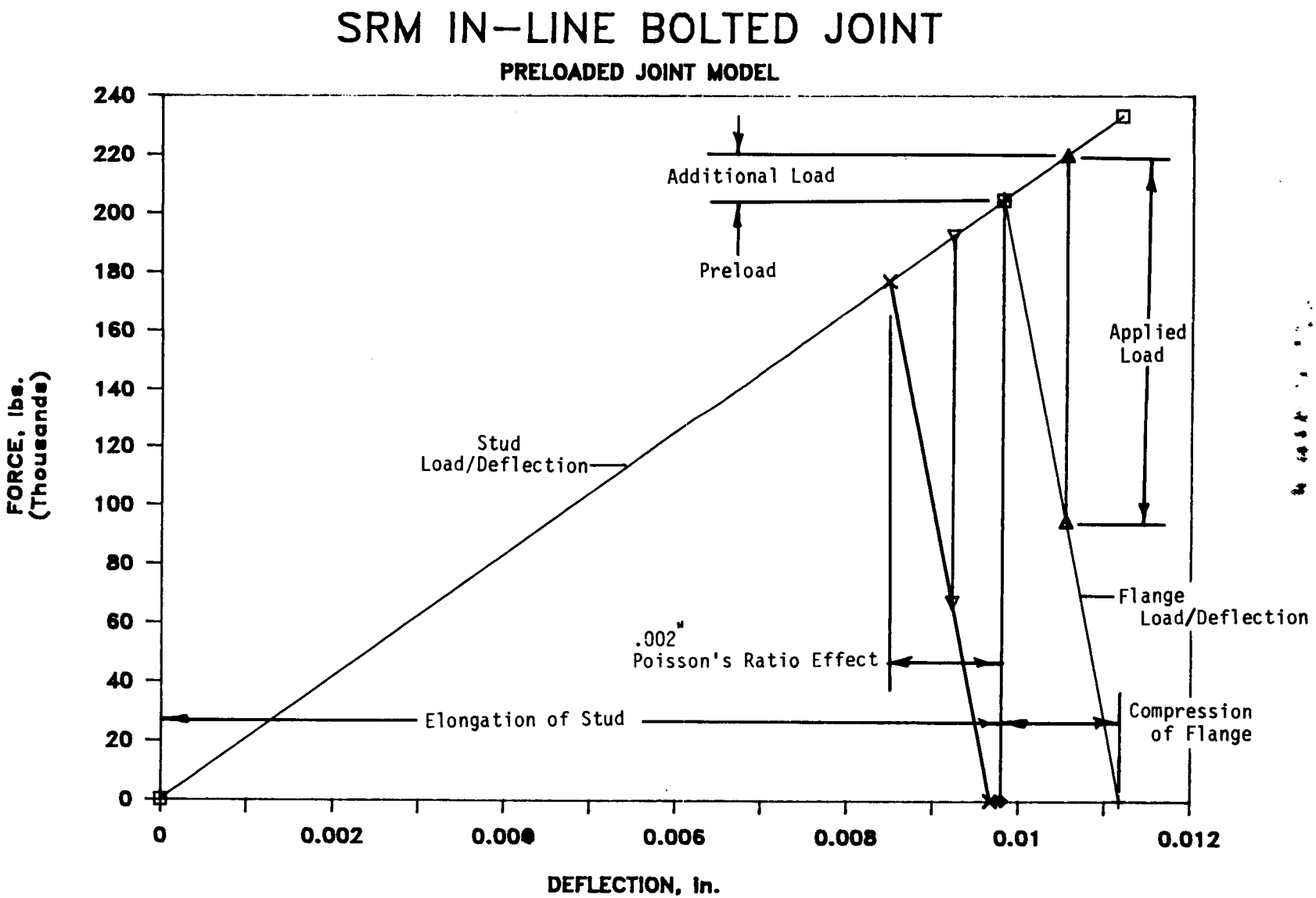

Figure 21. Preloaded bolt model.

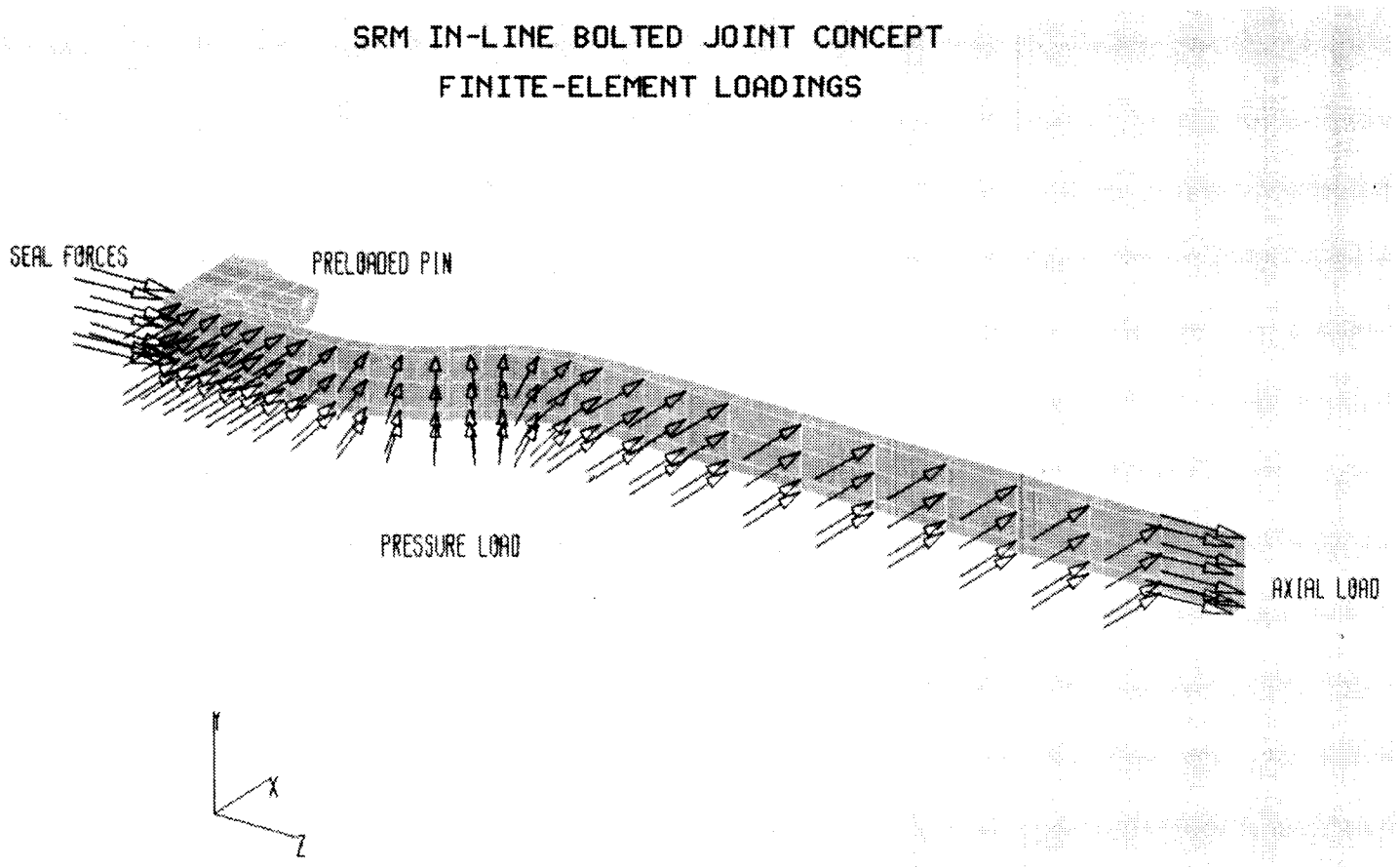

Figure 22. In-line bolted joint concept finite-element loadings.

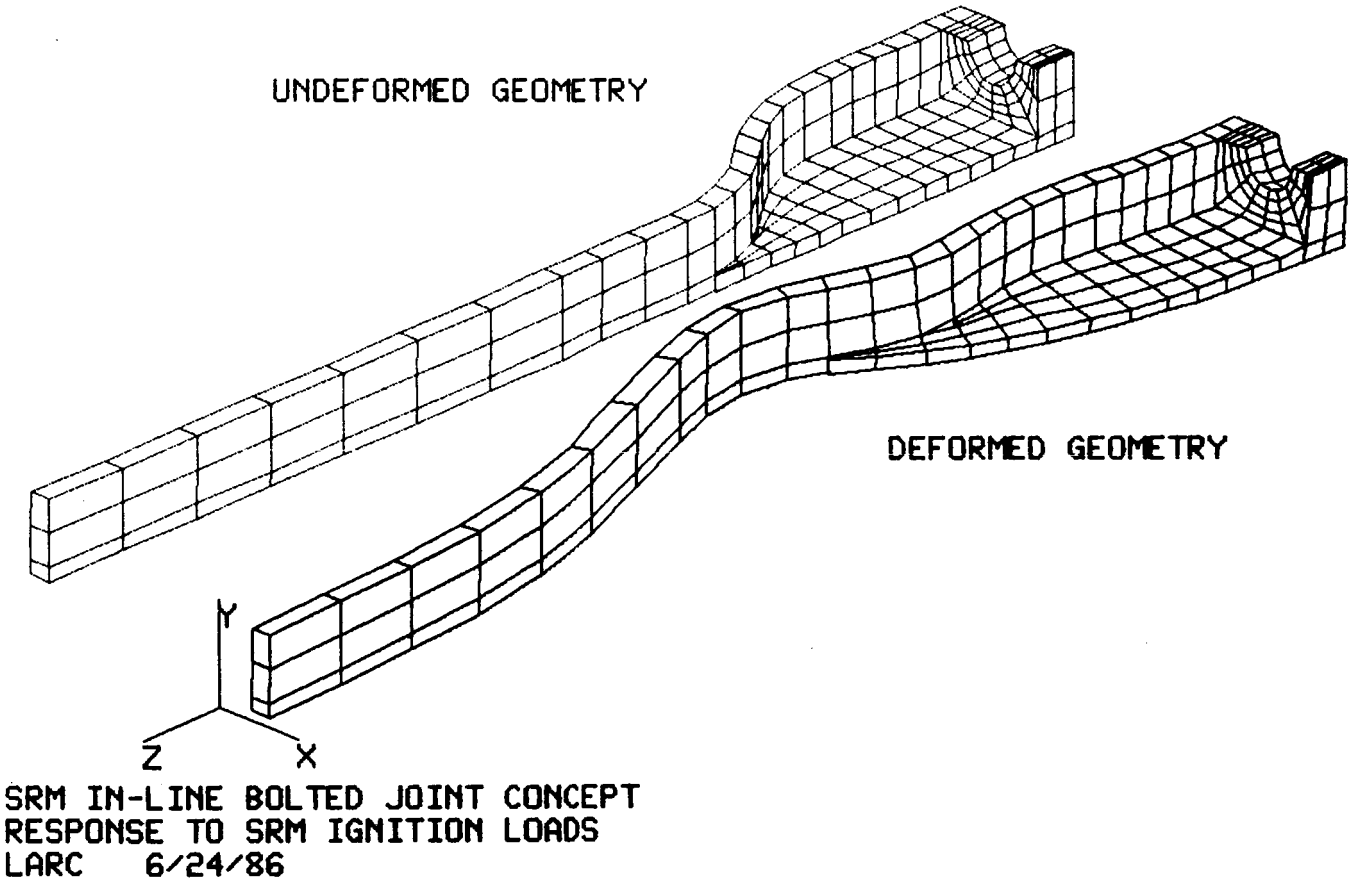

Figure 23. Undeformed/deformed geometry.

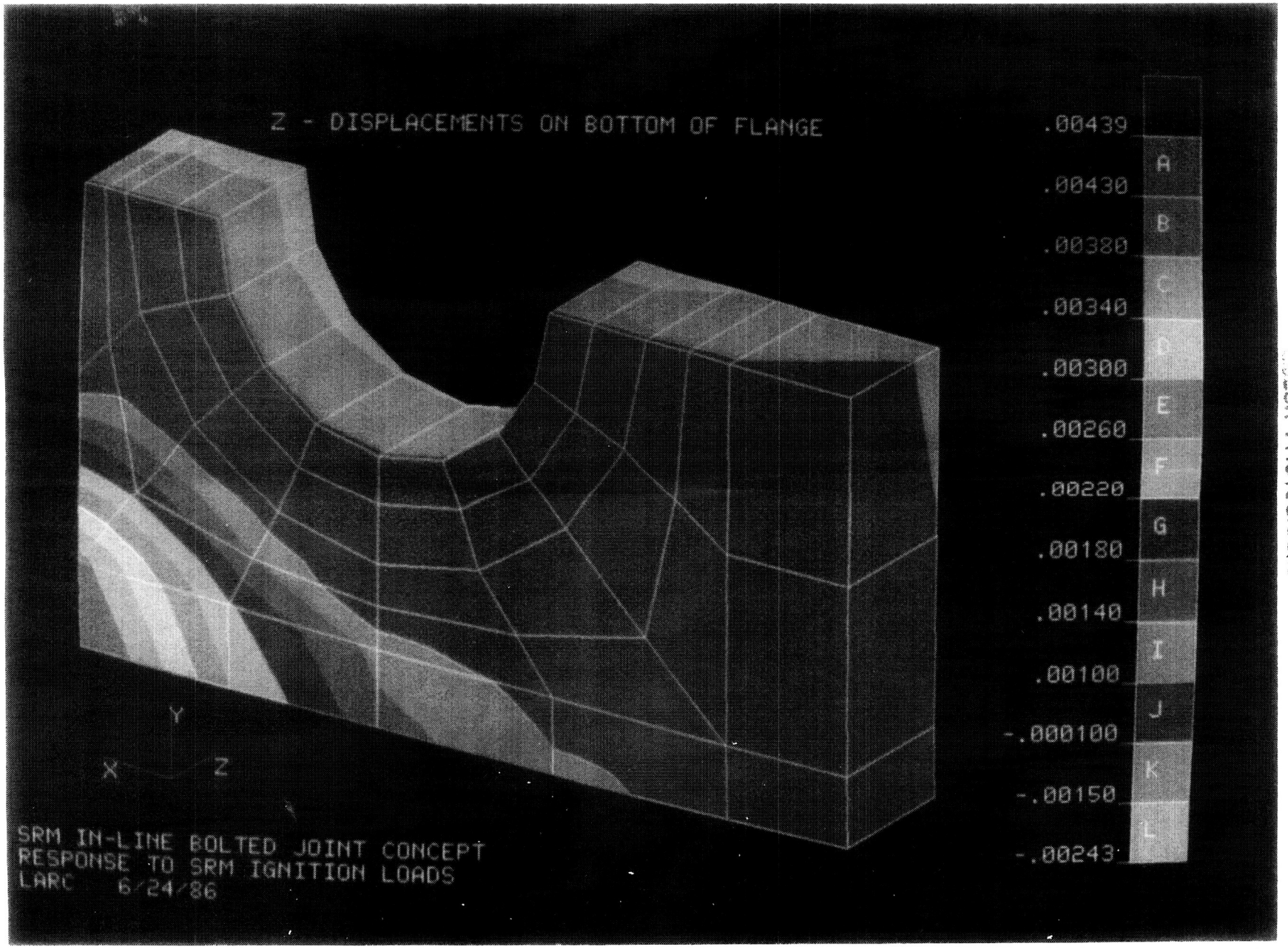

Figure 24. Z-displacements on bottom of flang (flang footprint).

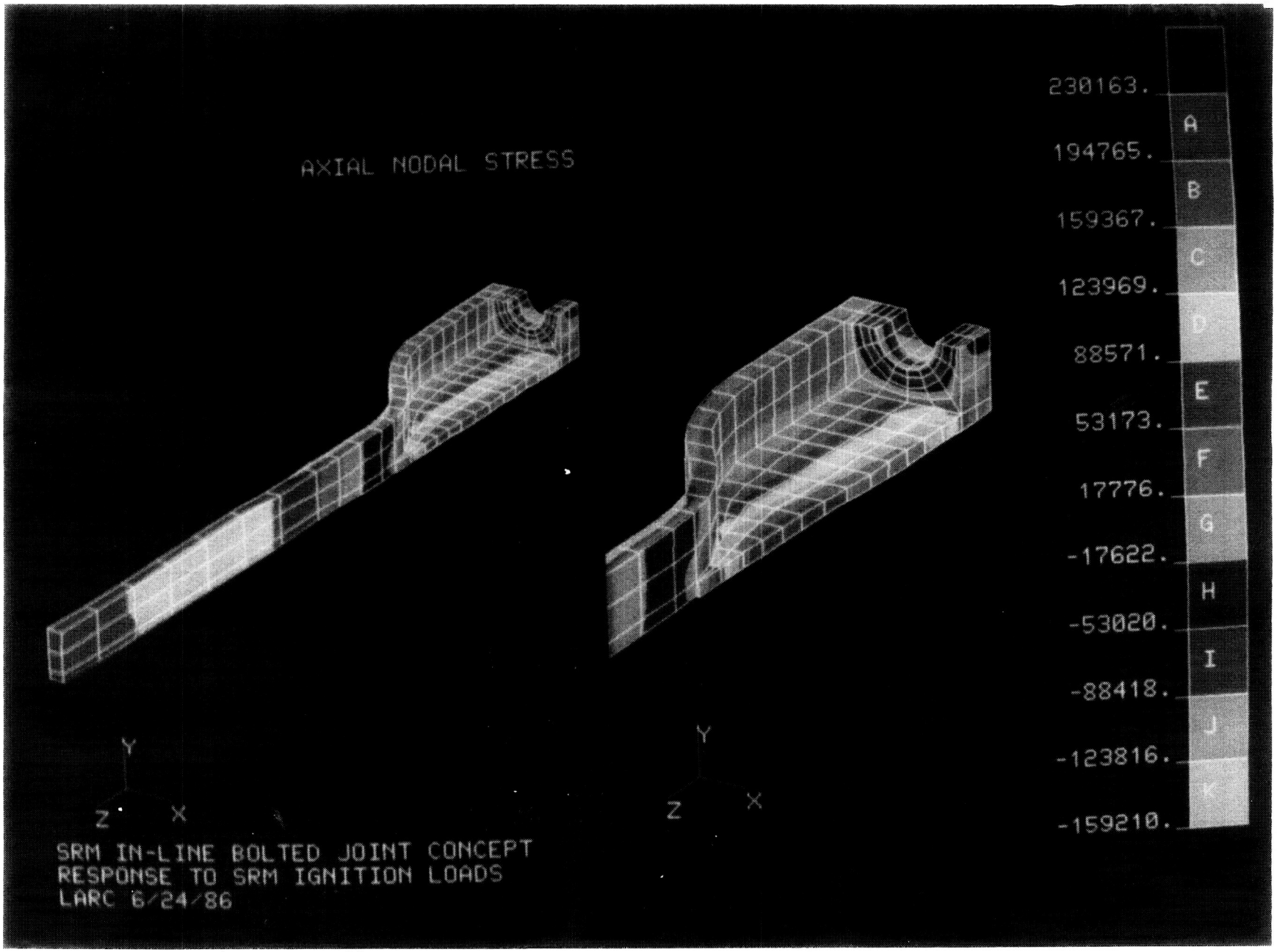

Figure 25. Axial nodal stress contours outside view.

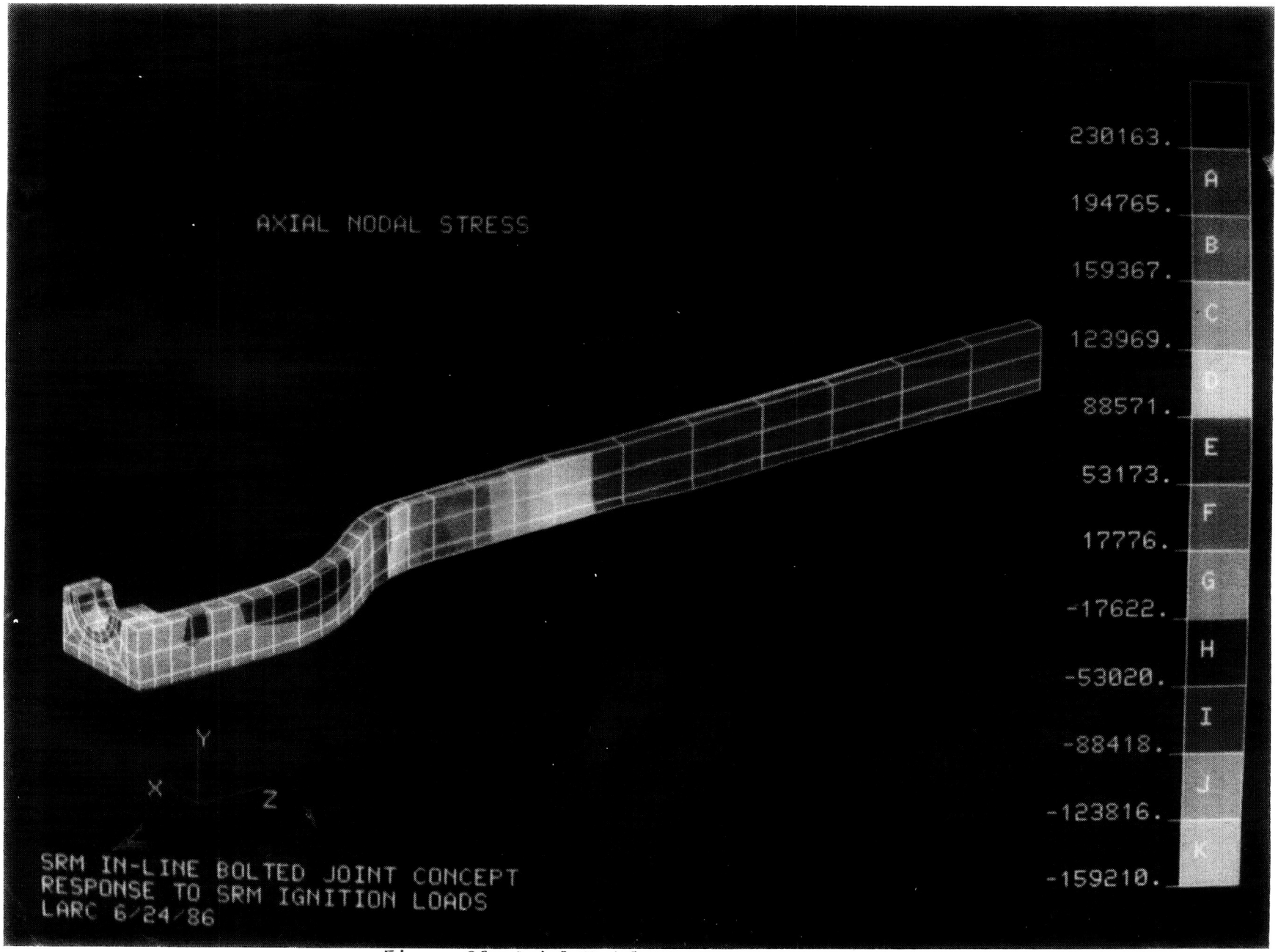

Figure 26. Axial Nodal stress contours inside view.

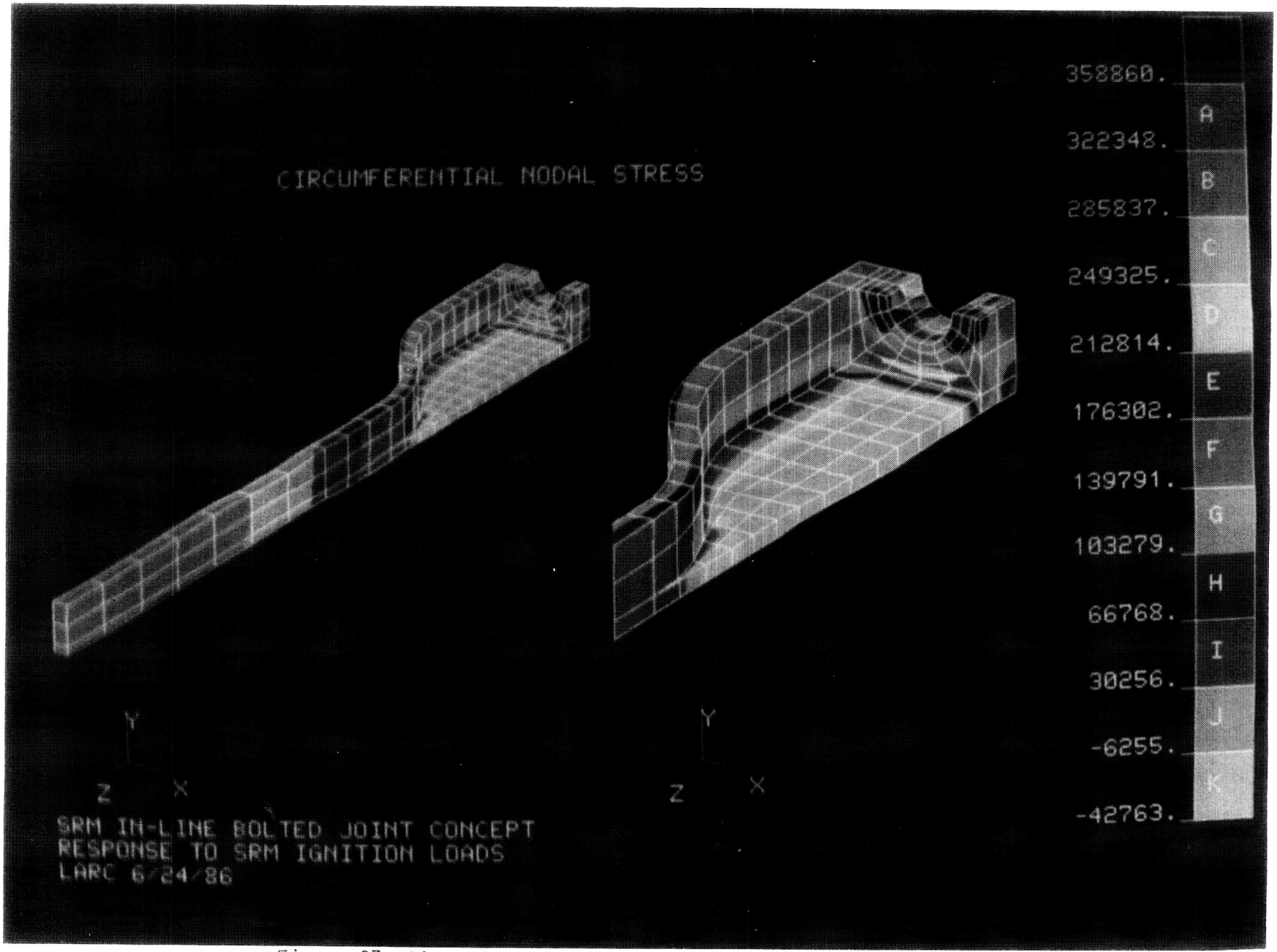

Figure 27. Circumferential nodal stress contours outside view.

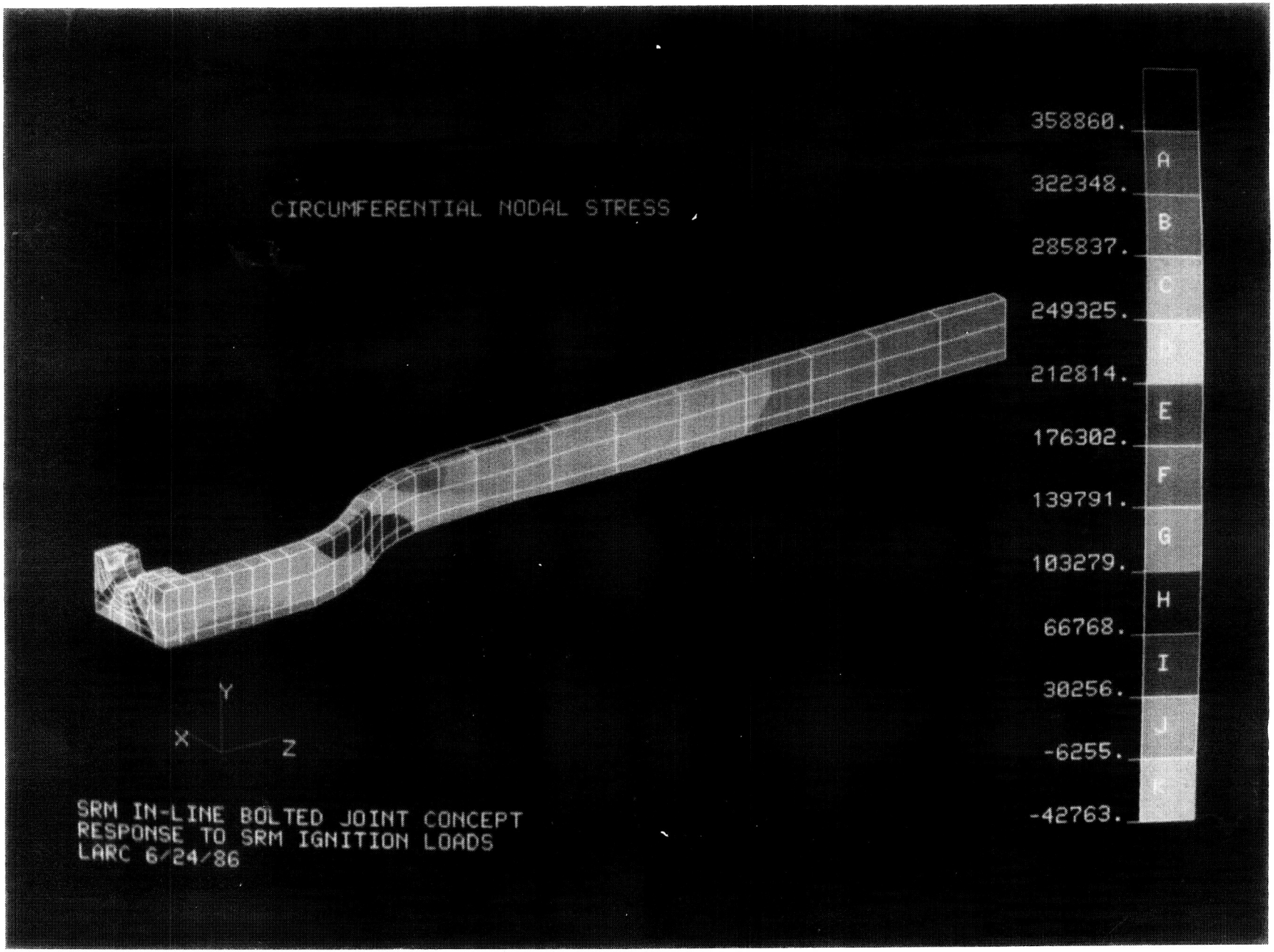

Figure 28. Circumferential nodal stress contours inside view.

SRB JOINT CIRCULARIZER

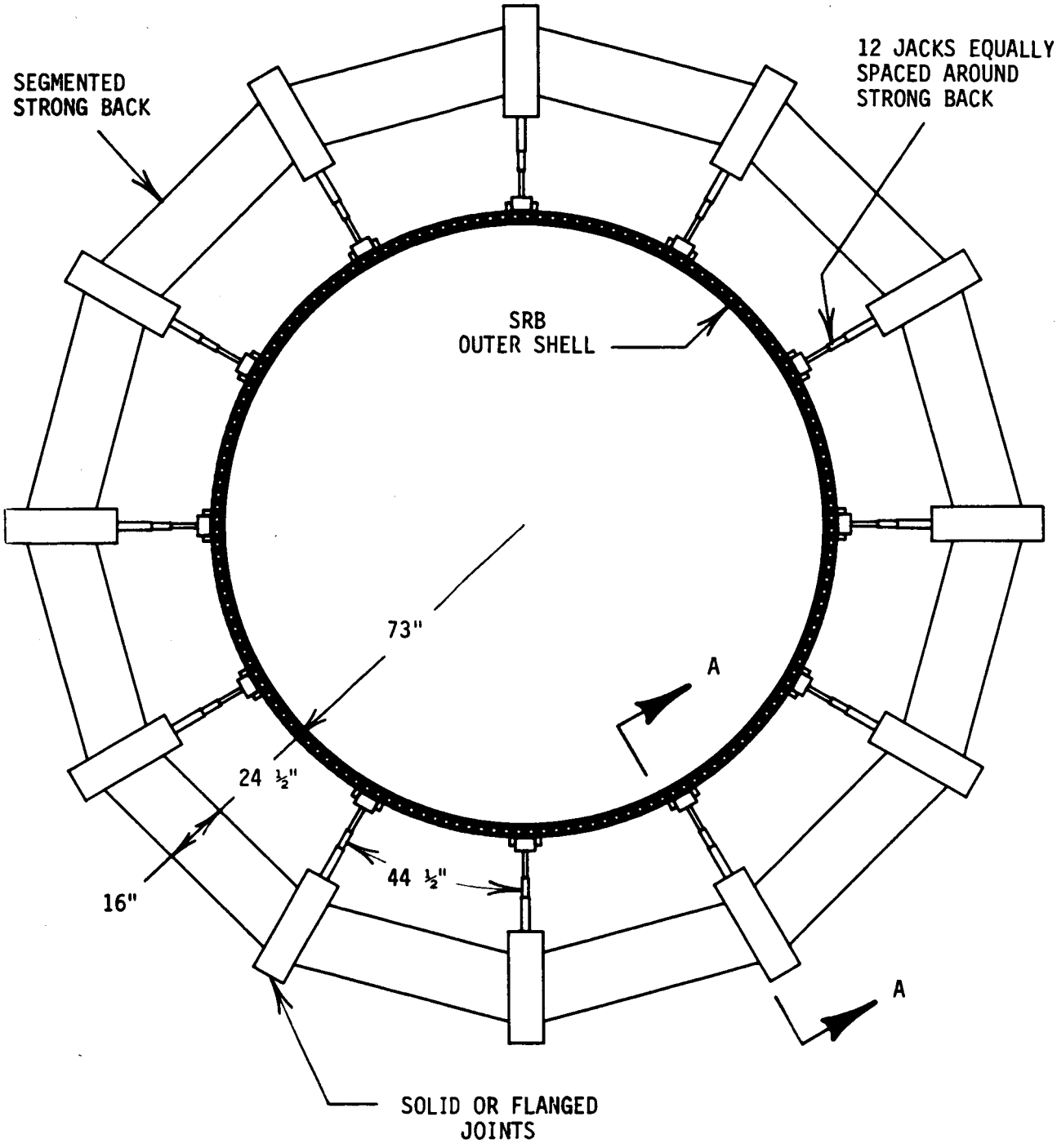

Figure 29.

SRB JOINT CIRCULARIZER

SECTION A-A

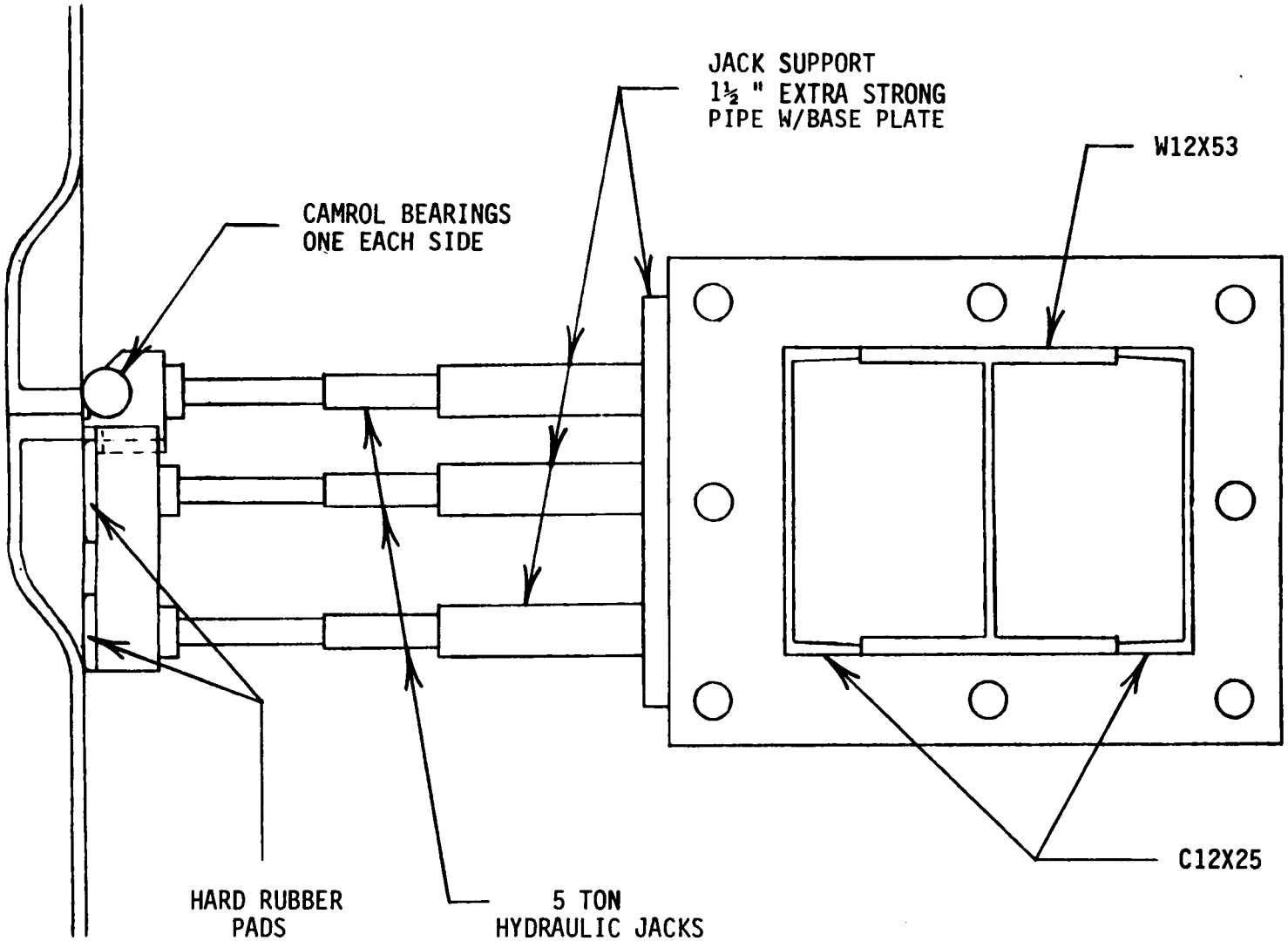

Figure 30.

ALIGNMENT PIN

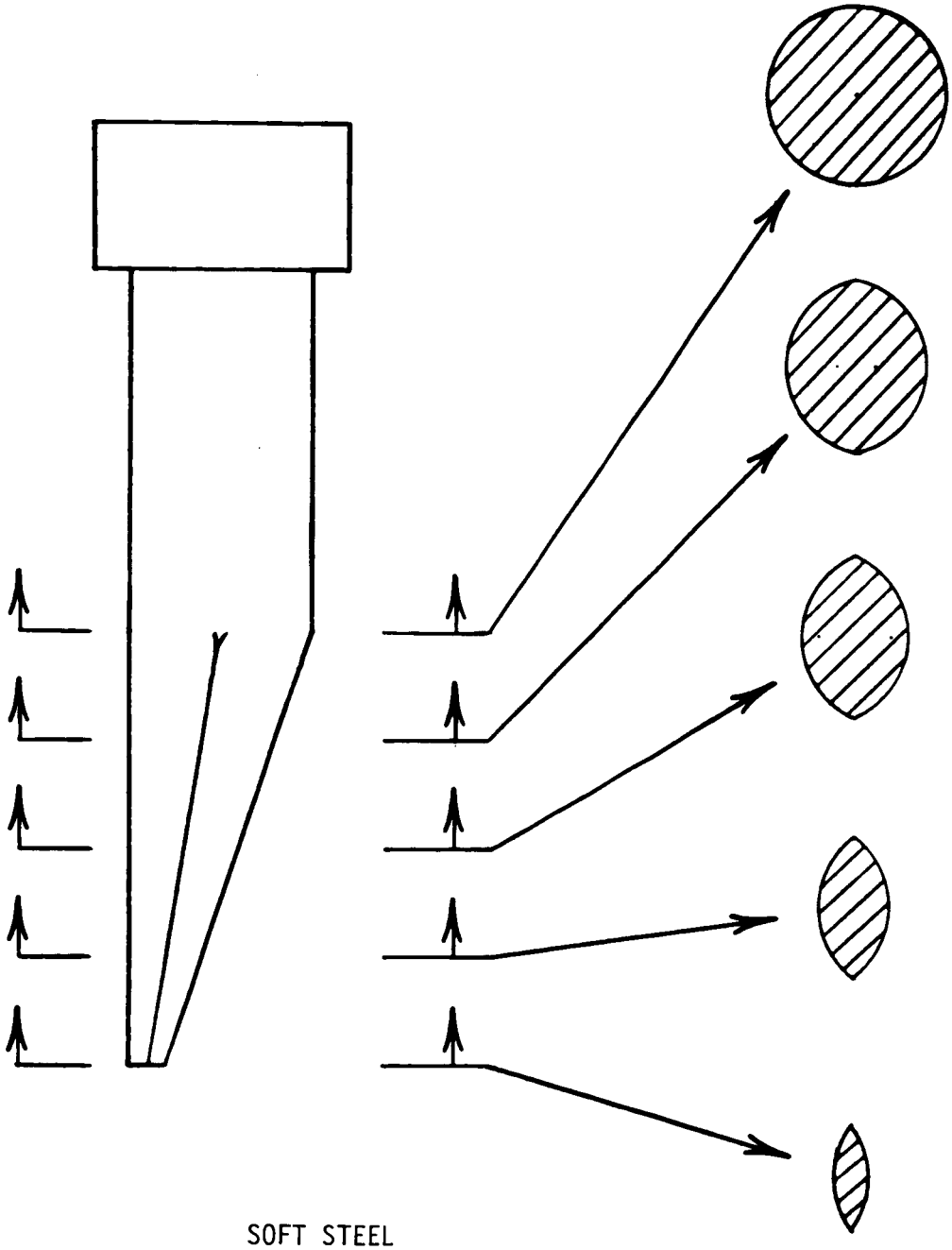

SOFT STEEL

Figure 31.

ASSEMBLY PROCESS

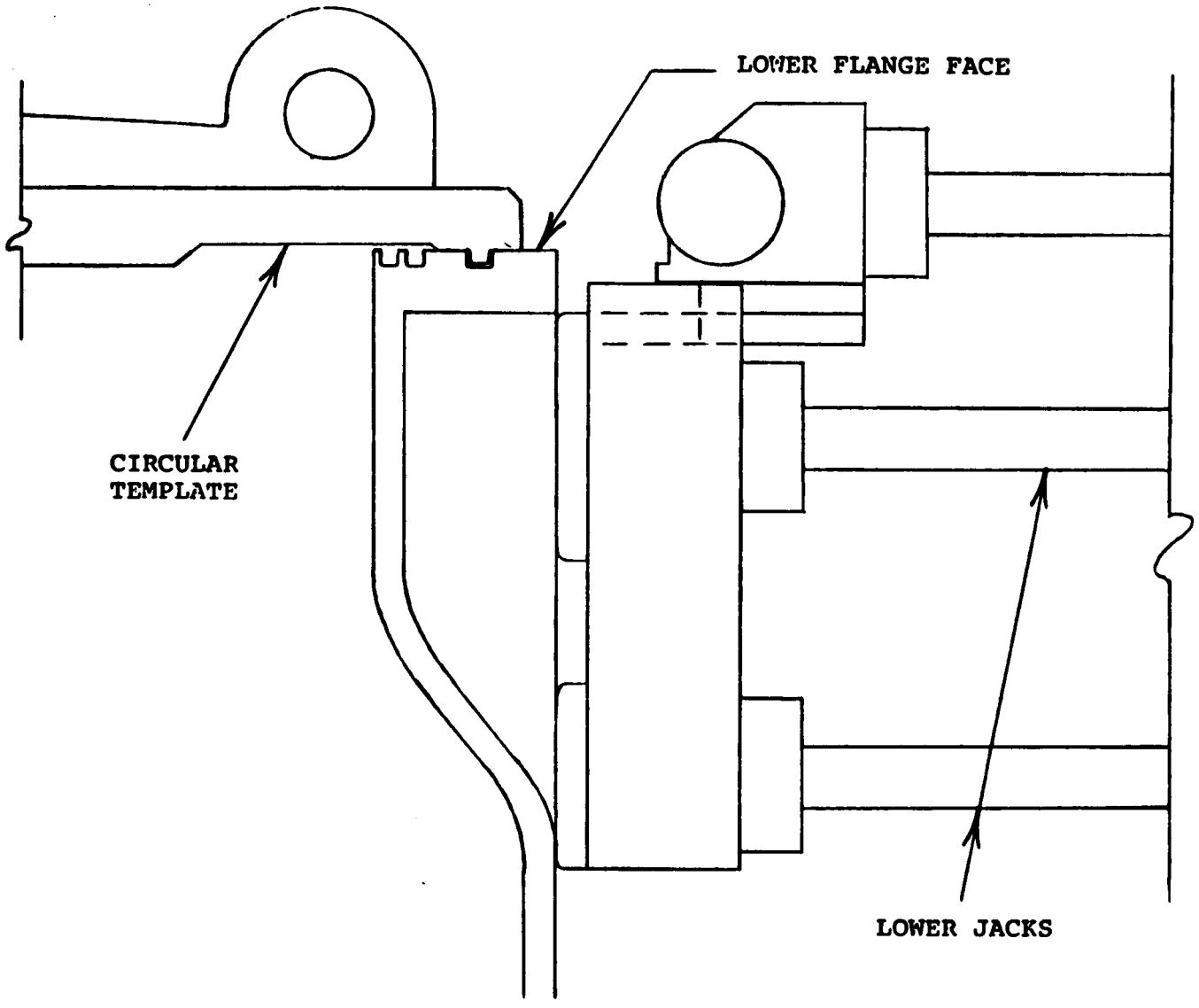

Figure 32.

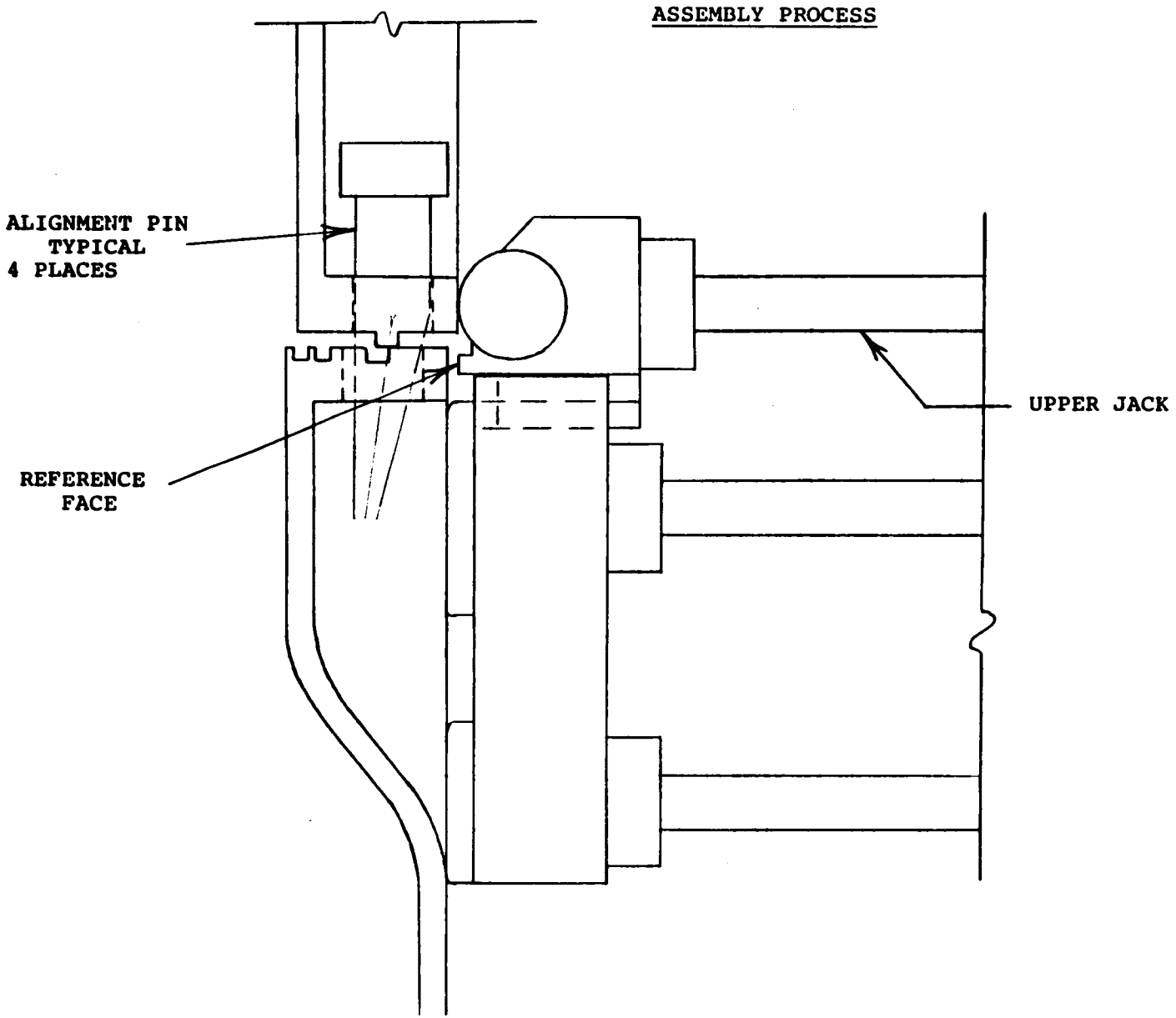
ASSEMBLY PROCESS
ALIGNMENT PIN
TYPICAL
4 PLACES
REFERENCE
FACE
UPPER JACK

Figure 33.

REFERENCES

1. Montano, J.: A Mechanical Property and Stress Corrosion Evaluation of MP35U Multiphase Alloy. NASA TMX-64591, 1971.

2. Anon: National "O" Rings Engineering Manual. Federal Mogul Corporation, 1982.

3. Carnahan, R.: Mechanical Testing of Silica Phenolic Composites at Elevated Temperatures. SAMPE Vol. 14, 1968.

4. Cullom, R.: Experimental Investigation of the Feasibility of Ablation-Cooling a Rocket Nozzle with Possible Application to Solid-Propellant Engines. NASA TM X-418, 1961.

5. Thomas, P.: Effects of Thermal Stabilization on the Properties of a High Temperature, Glass Reinforced Phenolic Molding Compound. Sandia Laboratories, SC-TM-70-716, 1965.

6. Petley, D. H.: Smith, D. M.: Edwards, C. L.: Carlson, A. B.: Analysis of Gap Heating to Stepped Tiles in Shuttle Thermal Protection System. NASA TP 2209, 1983.

Standard Bibliographic Page

1. Report No.	2. Government Accession No.	3. Recipient's Catalog No.
NASA TM-89046		

4. Title and Subtitle	5. Report Date
LaRC Conceptual Design of Solid Rocket Booster In-Line Bolted Joint	December 1986
	6. Performing Organization Code: 506-43-41-04
7. Author(s)	8. Performing Organization Report No.
9. Performing Organization Name and Address: NASA Langley Research Center, Hampton, VA 23665-5225	10. Work Unit No.
	11. Contract or Grant No.
12. Sponsoring Agency Name and Address: National Aeronautics and Space Administration, Washington, DC 20546-0001	13. Type of Report and Period Covered: Technical Memorandum
	14. Sponsoring Agency Code

15. Supplementary Notes

16. Abstract

An alternate STS Solid Rocket Booster (SRB) joint has been designed to perform safely and reliably under STS launch conditions. All design requirements for the SRB have been considered in addition to an evaluation criteria developed by LaRC to assess other candidate designs. Two primary objectives were to design an SRB pressure shell sealing system that would be seated at assembly, and remain seated, and also be protected from the hot internal gases during burning. An interdisciplinary team was formed and the resulting design is a bolted in-line flanged joint sealed with an elastomeric "O" ring and a metal "C" ring. Flange gapping at the sealing surface is prevented by recessing the preloaded bolts to provide a compression load directly on the flange (at the sealing interface). Internal hot gas protection is provided to the joint by compressing a soft elastomer seal between rigid rings bonded to the pressure shell.

The redesign, manufacturing, and verification testing does not represent a major technical problem and the joint can be further optimized for weight reduction.

17. Key Words (Suggested by Authors(s))	18. Distribution Statement
Space transportation system Solid Rocket Booster In-Line flanged bolted joint metallic "C" seal	Unclassified - Unlimited Subject Category 02

19. Security Classif.(of this report)	20. Security Classif.(of this page)	21. No. of Pages	22. Price
Unclassified	Unclassified	88	A05

For sale by the National Technical Information Service, Springfield, Virginia 22161